Naval Research Laboratory
Washington, DC 20375-5000

NRL Memorandum Report 6272

Approximation of Viscoelastic Stresses from Newtonian Turbulent Kinematics

J. V. LAWLER, E. W. HENDRICKS, R. A. HANDLER AND R. I. LEIGHTON

Center for Fluids/Structure Interactions Branch
Laboratory for Computational Physics and Fluid Dynamics

September 1, 1988

SECURITY CLASSIFICATION OF THIS PAGE

REPORT DOCUMENTATION PAGE

Form Approved OMB No. 0704-0188

1a. REPORT SECURITY CLASSIFICATION UNCLASSIFIED	1b. RESTRICTIVE MARKINGS
2a. SECURITY CLASSIFICATION AUTHORITY	3. DISTRIBUTION/AVAILABILITY OF REPORT Approved for public release; distribution unlimited.
2b. DECLASSIFICATION/DOWNGRADING SCHEDULE	
4. PERFORMING ORGANIZATION REPORT NUMBER(S) NRL Memorandum Report 6272	5. MONITORING ORGANIZATION REPORT NUMBER(S)
6a. NAME OF PERFORMING ORGANIZATION Naval Research Laboratory 6b. OFFICE SYMBOL (If applicable) Code 4420	7a. NAME OF MONITORING ORGANIZATION
6c. ADDRESS (City, State, and ZIP Code) Washington, DC 20375-5000	7b. ADDRESS (City, State, and ZIP Code)
8a. NAME OF FUNDING/SPONSORING ORGANIZATION Office of Naval Research 8b. OFFICE SYMBOL (If applicable)	9. PROCUREMENT INSTRUMENT IDENTIFICATION NUMBER
8c. ADDRESS (City, State, and ZIP Code) Arlington, VA 22217	10. SOURCE OF FUNDING NUMBERS PROGRAM ELEMENT NO: 61153N; PROJECT NO:; TASK NO: RR023-01-41; WORK UNIT ACCESSION NO: DN158-015

11. TITLE (Include Security Classification)
Approximation of Viscoelastic Stresses from Newtonian Turbulent Kinematics

12. PERSONAL AUTHOR(S)
Lawler, J.V., Hendricks, E.W., Handler, R.A. and Leighton, R.I.

13a. TYPE OF REPORT	13b. TIME COVERED	14. DATE OF REPORT (Year, Month, Day)	15. PAGE COUNT
Interim	FROM 4/86 TO 4/88	1988 September 1	57

16. SUPPLEMENTARY NOTATION

17. COSATI CODES			18. SUBJECT TERMS (Continue on reverse if necessary and identify by block number)
FIELD	GROUP	SUB-GROUP	Drag reduction; Turbulence; Non-newtonian

19. ABSTRACT (Continue on reverse if necessary and identify by block number)

A report on work conducted in the area of non-Newtonian turbulent kinematics. A summary of rheological measurements in turbulent non-Newtonian flows is given. A technique for approximating non-Newtonian viscoelastic stresses from Newtonian kinematics obtained by direct numerical simulation is presented.

20. DISTRIBUTION/AVAILABILITY OF ABSTRACT	21. ABSTRACT SECURITY CLASSIFICATION
☒ UNCLASSIFIED/UNLIMITED ☐ SAME AS RPT ☐ DTIC USERS	UNCLASSIFIED
22a. NAME OF RESPONSIBLE INDIVIDUAL Eric W. Hendricks	22b. TELEPHONE (Include Area Code) (202) 767-2516 Code 4420

DD Form 1473, JUN 86 Previous editions are obsolete

S/N 0102-LF-014-6602

CONTENTS

APPROXIMATION OF VISCOELASTIC STRESSES FROM NEWTONIAN TURBULENT KINEMATICS

INTRODUCTION

Experimentally, it has been determined that small amounts of high molecular weight polymers (a few parts per million by weight) dissolved in a solvent can reduce the turbulent flow frictional resistance of that solution by 75 percent. Since the viscosity of a polymer/solvent mix is increased over that of the solvent alone, the fact that viscous drag is decreased is somewhat surprising. The study of drag reducing, non-Newtonian fluid flows received its initial impetus from the work of Toms (1948). Since Toms, the examination by fluid dynamicists of the turbulent flow properties of thermodynamically dilute solutions of long chain high-molecular weight polymers has generated literally hundreds of publications, of which a majority are experimental investigations. This preponderance of experimental studies is no doubt due to the difficult theoretical nature of the problem, which includes not only turbulence but the interaction of a viscoelastic fluid with turbulence. The study of viscoelastic fluids as they relate to drag reduction is itself an area of investigation among rheologists. Several excellent reviews of the available experiments and possible explanations of this phenomenon have been conducted since Toms original work: Lumley (1969) and (1973), Hoyt (1972), Virk (1975), Little *et al.* (1975), and Berman (1978). The reader is referred to Lumley (1973), Berman (1978) and a recent work by Ryskin (1987a) for theoretical discussions of the drag reduction phenomenon. This paper is in two sections. In the first section, we review the rheological properties of dilute polymer solutions. In the second section, we present a method for approximating viscoelastic stresses in a turbulent flow.

* Presently at Hoechst Celanese Research Division, Summit, NJ 07901.

Manuscript approved May 14, 1988.

Rheological Characterization of Drag Reducing Fluids

In this section, we discuss the measurements of the rheological properties of dilute polymer solutions as they relate to turbulent flow drag reduction. The flow of a viscoelastic polymer solution is markedly different in many ways from its Newtonian counterpart. These differences are due to the long chain structure of polymers. The flow properties of viscoelastic fluids are often rate-dependent. Once a threshold strain rate has been exceeded the shape of the polymer molecule becomes anisotropic and partially aligns with the flow. This anisotropy produces stresses along the backbone of the aligned molecule. In shearing flows, components of the anisotropic stresses in a viscoelastic fluid that act in a direction normal to the deformation gradient are, not surprisingly, called "normal" stresses. The large number of atoms in a polymer molecule allow large deformations. The time required for a polymer to diffuse back to equilibrium is many orders of magnitude greater than the corresponding relaxation times of Newtonian fluids. Consequently, polymer solutions have relaxation times from milliseconds to seconds. Finally, the stresses in a polymer solution are a function of the previous deformations of the fluid, since these deformations have altered the current conformation of the polymers. This dependence on past events is termed "memory".

We will begin with a section on constitutive equations. Followed by a discussion of extensional viscosity and its relation to a drag reduction mechanism. A discussion will be presented on rheologists attempts to quantify some of the constants in the consititutive equations and to predict turbulent flow modifications. The effects of entanglements and degradation on drag reduction measurements will be examined. Finally, a discussion of some important recent research and aims for the future.

Constitutive Equations

Constitutive equations are mathematical expressions which model the stress level and distribution in a polymer solution or melt (see recent books by Tanner 1985, Bird *et al.* 1987a & 1987b, and Larson 1988). The validity of the many proposed

constitutive equations as accurate models for dilute polymer solutions in a turbulent flow is largely untested, because the state of polymers in turbulent flows is so poorly understood. Consequently, many of the assumptions invoked to develop a specific constitutive equation cannot be tested. Since a plethora of constitutive equations exist and turbulent flow is extremely complex, these equations have historically been tested in simple but relevant flows. Measurements of stresses, velocities, orientations, or geometry-specific flow parameters can also be conducted in these simpler flows for the independent determination of some or all of the constants or functions which appear in a constitutive equation.

Elongational Properties

Elongational viscosity is defined as the constant of proportionality between the difference of the spanwise and the axial normal stresses and the elongation rate. The modifications of turbulent flow, cavitation, and other flow instabilities by polymer solutions is the result of the high elongational viscosity of dilute polymer solutions (Ting and Hunston 1977). On a unit concentration basis, the magnitude of the effect increases with decreasing concentration. From this observation, Ting and Hunston postulate that the large elongational viscosity is a polymer-solvent and not polymer-polymer interaction because there are ten billion to one trillion solvent molecules for each polymer molecule in these dilute solutions. It is unfortunate that the measurements of this important property remain uncertain. The methods used to obtain an estimate of the elongational viscosity are discussed below.

The excess pressure required to force a dilute polymer solution through an orifice is the result of the high elongational viscosity of these solutions. This flow geometry is presented in Figure 1. To obtain an order of magnitude estimate of the elongational viscosity, Fruman and Barigah (1982) utilize data from an orifice flow with the assumption that the elongational viscosity is a constant and independent of strain or strain rate. These analyses indicate that the elongational viscosity is several orders of magnitude larger than the shear viscosity.

Fiber spinning and a ductless syphon have been employed to measure the elongational viscosity of dilute solutions. The fiber-spinning and ductless syphon geometries are depicted in Figures 2 and 3, respectively. By assuming an absence of radial gradients and measuring the force along the fluid, the elongational stresses and elongational viscosities can be calculated from photographs taken of the profile of the fluid. As with orifice flow, the measured elongational viscosities of solutions are found to be about three orders of magnitude larger than the shear viscosities (Weinberger & Goddard 1974 and Usui & Sano 1981). The durations of the elongations in fiber spinning/ductless syphon experiments are too short to produce steady-state stresses in the solutions, although this assumption is routinely made in the analyses.

Attempts have been made to minimize the errors in the measurement of elongational properties. Baid and Metzner (1977) have calculated the response of various fluid models to the time-dependent strain history occurring along the length of a fiber to simulate more accurately the stress history. Recent work by Matthys (1987) has shown that radial gradients do exist and that the axial velocity on the outer surface is greater than at the core. Becraft and Metzner (1988) discuss methods to reduce other sources of errors in making measurements during a fiber-spinning experiment.

Most constitutive equations predict this elongational viscosity. Chakraborty and Metzner (1986) have been able to simulate qualitatively the orifice flow experiments of James and Saringer (1982) by calculating the stresses in the flow with an Oldroyd-B fluid model. Ryskin (1987b) has also been able to simulate these same excess pressure drop experiments with his "Yo-Yo" model, which he has also used to predict some aspects of turbulent drag-reduction (Ryskin 1987a). As interesting as these predictions are they are really only of value if they can be extended to other flows. Baid and Metzner (1977) have been able to model shear and elongational flows with the Oldroyd-B model but, only by selecting a different set of parameters for each flow.

An important tool in the measurement of the rheological properties is flow birefringence, which allows the stress and its orientation to be determined optically (Lodge

1955, Philippoff 1956, and Brodnyan *et al.* 1957). Dandridge *et al.* (1979) have measured the birefringence of an aqueous solution of PEO over a concentration range of 50 to 1350 *ppm* in a shear flow above a shear rate of 2000 s^{-1}. The birefringence of polymer solutions has been measured in elongational flow with the the crossed-slots and opposed-jets geometries. Schematic diagrams of these geometries are shown in Figures 4 and 5. In these experiments the extension rate at which the polymers begin to uncoil and hence to show strong birefringence can be determined. In the small regions of these flows undergoing elogational deformations, once uncoiling begins it is expected that the polymer will completely extend, if the residence time is sufficiently long (DeGennes 1974). This complete extension produces the strong birefringence in a small region of the flow domain. Keller and Odell (1985) demonstrate that birefrigence in crossed slots can also be used to measure the molecular weight distribution of polymers. The technique is especially accurate for measuring the high molecular weight tail, which is difficult to obtain by standard methods. At a flow rate above the onset of birefringence a second birefringence phenomenon appears, which consists of a large area of birefringence within the flow domain (flaring). Researchers interpret this second transition as the elongation rate at which interconnected polymer chains cannot disentangle in time to deform principally as isolated chains (Odell *et al.* 1985).

The four-roll mill is another useful rheological tool. It can be used to examine the effect of elongational deformations on polymer solutions. The deformation history with counter-rotating rollers in a Newtonian fluid is close to an ideal hyperbolic flow (Crowley *et al.* 1976). The principal limitations of this device are that high elongation rates cannot be obtained at low Reynolds number. The stresses in a dilute solution of polystyrene (PS, 50-100 *ppm*) in a viscous solvent is reported by Fuller and Leal (1980) in this geometry. The birefringence levels observed during elongation are three to four orders of magnitude higher than those observed previously in shear flows at comparable deformation rates. They are able to model closely the birefringence and stresses of this PS solution with a dumbbell model which included a nonlinear hydrodynamic friction, an internal viscosity, and a molecular weight distribution.

Shear Viscosity and Normal Stresses

Shear viscosity (hereafter referred to as simply "viscosity") is the easiest rheological property of dilute solutions to measure accurately. The "ease" with which the viscosity of dilute polymer solutions can be measured is more a consequence of the difficulty in measuring other rheological properties. Most standard rheological techniques for measuring non-Newtonian viscosities cannot be used with dilute aqueous solutions due to the low viscosity of water. Further complications are the significant non-Newtonian entrance effects (Bagley 1957) and adsorption-entanglement layers (Hikmet *et al.* 1985) that develop in capillary rheometers, which are the rheometers most often used to characterize dilute solutions. However, it can be reliably stated that the viscosities of aqueous dilute solutions of polymers (less than 200 ppm) are less than ten percent higher than the viscosities of the solvents.

The most important change in the viscosity of a non-Newtonian fluid is that the viscosity becomes a function of shear rate. The combination of a relative viscosity close to unity and a low solvent viscosity makes determining the viscosity of dilute polymer solutions as a function of shear rate difficult with current rheometers. The relative viscosity is the ratio of the solution viscosity to the solvent viscosity. The viscosities of these solutions are only very weak functions of shear rate. Hoyt and Fabula (1964) have measured no change in viscosity for polyethylene oxide solutions (PEO, Union Carbide WSR-301) ranging in concentration from 10 to 100 *ppm* up to a shear rate of 500,000 s^{-1}. Belokon *et al.* (1973) have reported that aqueous solutions of PEO (WSR-301) only begin to depend on shear rate above a concentration of 200 *ppm*. Solutions with concentrations less than 100 *ppm* are the critical fluids for testing drag reduction theories; these solutions are the most efficient drag-reducers. Hoyt (1971) finds that the minimum concentration required to reach the maximum drag reduction asymptote is only 20 to 30 *ppm* for an aqueous PEO (WSR-301) solution, with a 2 to 4 *ppm* solution producing one-half of the maximum reduction.

The lack of significant shear thinning (the reduction of viscosity with increasing

shear rate) of the strongly drag-reducing solutions cited above demonstrates that shear-thinning is not the principal mechanism for drag reduction. Further evidence is reported by Hoyt and Fabula (1964). They have measured no reduction in turbulent drag for a carboxy vinyl polymer (Carbopol 941) solution, which is shear-thinning but inelastic.

Finally, very few measurements of the normal stresses of these fluids have been reported for the same reasons that the viscosity as a function of shear rate curve is difficult to determine for dilute aqueous solutions. However, normal stresses of more concentrated solutions can be measured. The magnitude of the normal stress is related to the relative viscosity of the solution. At higher concentrations (that is, high relative viscosities), the normal stresses can be separated from the shear stress and other sources of noise.

Relaxation Times From Shear Measurements

The relaxation time of a polymer solution represents the time scale over which deformed polymer conformations return to equilibrium conformations. Baid and Metzner (1977) have measured the viscosity and normal stresses for a 100 *ppm* polyacrylamide (PAC, Dow Separan AP-30) in a glycerin/water solution. They have estimated the Maxwell relaxation time (normal stress divided by twice the shear stress and shear rate) to be about 50 *ms*. Darby and Chang (1984) have measured the shear rate at which the viscosity decreases for PAC (AP-30) in water. The reciprocal of this critical shear rate is another estimate of the relaxation time for a viscoelastic fluid. Darby and Chang's estimate is about 10 to 20 *s* for a 100 *ppm* solution. A disagreement of 3 orders of magnitude.

The relaxation time, from linear viscoelastic theory, is linearly proportional to the viscosity of the solvent, if one neglects the change in the intrinsic viscosity due to a change in the solvent (Rouse 1953). Therefore, the differences in relaxation times discussed above may be be even greater if measured in the same solvent. The ambiguity and uncertaintity of shear measurements in dilute solutions make determining relax-

ation times and other consitutive equation parameters from shear flow measurements inadvisable.

Relaxation Time Based On Elongational Flow

The reciprocal of the critical extension rate is equal to twice the relaxation time of the polymer molecule. Farrell *et al.* (1980) find that the relaxation time and the dependence of that time on molecular weight of a 2500 ppm solution of polystyrene agrees with the Zimm molecular model for a non-free draining molecule (Zimm 1956). James and Saringer (1982) measure a relaxation time in their orifice experiments for a PEO solution. The measured relaxation time is different from the Zimm model relaxation time by a factor of three. The discrepancy in these two results reported for the orifice geometry is probably due to the uncertainty in determining the elongation rates occurring in this geometry. Optical techniques could be used to determine elongation rates.

Mixed Flows

Turbulent flows are combinations of shear and elongational deformations. Recent analysis of the numerical simulations of wall-bounded Newtonian turbulence by ourselves (Lawler *et al.* 1987) finds that the shear component of deformation near the wall is large enough to enhance the resistance to elongation (increase elongational viscosity) for a large class of fluid models. It is critical that fluid models be tested in at least mixed laminar flows. Recent experimental results for flow into an orifice by James and his co-workers (1987) demonstrate that preshearing of the fluid before it enters an orifice has a profound effect on the excess pressure drop. One explanation is that a deformed polymer molecule is much more rapidly elongated than a molecule in its equilibrium configuration. Another explanation is that networks form during the shearing, and these structures require higher stress levels to deform in an elongational flow than do individual molecules. The effect of preshearing might be predicted by an

Oldroyd-B or "Yo-Yo" model if this new complex flow were simulated. However, the analyses by Chakraborty & Metzner (1986) and Ryskin (1987b) must be expanded to at least two-dimensional flow problems if preshearing or other more realistic kinematics are to be modelled.

The aforementioned, four-roll mill is an excellent geometry in which to study complex flows. A wide range of deformations, between pure elongation and simple shear, can be generated by varying the ratio of the angular velocities of the rollers. As discussed above, Fuller and Leal (1980) predicted the birefringence of a PS solution for both pure elongation. They obtained equally accurate predictions of the birefringence in mixed flows with their model. Dunlap and Leal (1987) extend the measurements in the four-roll mill to a wider range of mixed flows. They then calculate the birefringence of several molecular models to determine which models are able to predict the flow behavior in these mixed flows. The model of Phan-Thien *et al.* (1984), which includes conformation-dependent, anisotropic friction and strain-inefficient rotation, fit the behavior of the polymer solutions better than molecular models without these features. The match to experiments is worsened if internal viscosity is added to the model developed by Phan-Thien *et al.* This work by Dunlap and Leal is an excellent example of how mixed flow experiments can and should be used to test and develop constitutive equations.

Simulation of Complex Flows

The direct numerical simulation of low-Reynolds number Newtonian turbulent flow is now possible with the advent of supercomputers. Currently, channel flows at Reynolds numbers of up to 3300 have been simulated. This value of Re is only about one-third the value of Re at which significant effects of the polymer occur (as found in our flow experiments described later in this chapter). To predict turbulent drag reducing flows, one must incorporate a non-Newtonian constitutive equation into the simulations. However, to date the determination of the polymer properties necessary to form an accurate constitutive equation has not been successful. An approach which

takes advantage of the comparison of experiments to large-scale simulations is required. The increasing power of computers makes feasible the simulation of continuum fluid models in complex geometries. Comparison of experiments with these calculations may be a better method of selecting fluid models and determining the parameters in these fluid models than trying to measure rheological properties of these fluids directly.

A good candidate for a coupled simulation/experimental approach might be a vortex flow. Balakirshnan and Gordon (1971) have observed experimentally that a vortex does not form during the draining (through an orifice) of a tank filled with a dilute polymer solution. Schematic diagrams of the differences between the flows of a Newtonian fluid and a polymer solution are shown in Figure 7. Later these researchers (Gordon and Balakrishnan 1972) show that the minimum concentration for vortex inhibition is close to the concentration to achieve maximum drag reduction in a pipe. A third study (Chiou and Gordon 1976) contains measurements of the axial velocity above the orifice as a function of position. They found that this velocity is reduced by an order of magnitude in going from the Newtonian fluid to the polymer solution.

Another possible model geometry for simulations is the flow around a vibrating rod in a larger cylinder (see Figure 8). Chang and Schowalter (1974) present experiments which show that the vortices which form in a polymer solution are rotating in the opposite direction than those which form in a Newtonian fluid. Small vortices (not shown on the figure) occur near the vibrating cylinder in a Newtonian fluid. Perturbation calculations by Chang and Schowalter (1979) show that in an Oldroyd-B fluid model these small vortices grow as the elasticity of the fluid is increased. Eventually, these vortices, which are rotating in the opposite direction than the larger vortices in a Newtonian fluid, fill the gap between the cylinders: and the original large vortices disappear. Thus, the fluid model has been able to predict the effect of the polymer solution on the flow field. The relaxation time of the polymer solutions used in this study are determined by fitting the flow behavior to the numerical simulations. Sufficient rheological data are unavailable to obtain an independent estimate. Vlassopoulos and Schowalter (1988) have continued to study the flow of dilute polymer solutions in this

geomety. In their new experimental apparatus, they measure the velocity field with a laser-Doppler velocimeter. Their numerical analysis includes the ability to calculate the velocity fields of more complex fluid models.

The onset of Taylor vortices between concentric rotating cylinders is another good choice for the comparison of the flows of dilute solutions and fluid models. The vortices are generated by an inertial instability in the flow which Taylor (1923) has accurately predicted for a Newtonian fluid using perturbation theory. Denn and his co-workers (Ginn & Denn 1969, Denn & Roisman 1969, Denn *et al.* 1971, and Sun & Denn 1972) have successfully compared experiments with polymer solutions and Second-Order Fluid model stability calculations to determine the rheological properties of the polymer solutions. For some of the polymer solutions, these rheological properties agree with properties measured by other more standard rheological measurements. Comparisons for other polymer solutions do not show agreement. Jones *et al.* (1973) discuss the sources and magnitudes of the errors in determining these rheological properties from comparing experiments with Second-Order Fluid stability calculations. Despite the large number of experiments to measure the onset of Taylor vortices in dilute polymer solutions, only Beard *et al.* (1966) and Deutsch & Phillips (1977) have calculated the onset of Taylor vortex flow for a fluid model with memory and elasticity. Belokon *et al.* (1973) find that the onset Reynolds number is not affected by the very dilute drag reducing solutions. Therefore, the other aspects of the secondary flow which are altered by the presence of the polymers (for example, the radial and axial velocities) must be measured to test the predictive capabilities of fluid models. These perturbation velocities can be measured accurately with a laser-Doppler velocimeter (Gollub & Swinney 1975 and Lawler 1986).

Entanglements

Another aspect of dilute polymer solutions that must be considered when examining their affect on tubulence is molecular entanglements. Flaring in the crossed slots and opposed jets experiments indicate that entanglements between polymer chains do

exist in these dilute solutions (Odell *et al.* 1985). The state of entanglements may also depend on previous flow history, so experiments limited to pure elongational flows examine conformations which are different than the conformations found in mixed flows. Time of measurement, disentanglement time, and critical overlap density are all important and interrelated. Virk *et al.* (1967) reports the mean radius of gyration of PEO (WSR-301) in water as 240 *nm*. In a 30 *ppm* solution, the average spacings between centers of polymer molecules are about 800 *nm*. The volume contained inside the radii of gyration is 15 % of the total volume. In a face-centered cubic arrangement of spheres, the sphere volume is 74 % of the total volume. Clearly, interactions between polymers even at this dilution are quite strong, especially since the radius of gyration is a statistical quantity and the strands of the polymer extend well beyond the calculated radius. The size of molecules (or aggregates) in solution has been estimated by comparing the Pitot tube errors between polymer solutions and solutions of small particles (Belokon *et al.* 1973). For PEO the volume concentration is estimated as being about three orders of magnitude larger than the weight concentration. As demonstrated by Kowalik *et al.* (1987), polymeric systems with strong intermolecular forces produce a further reduction in the drag over that which is observed with similar systems but without strong interactions. In their four-roll mill geometry, Dunlap and Leal (1987) find that the volume fraction of the solution (based on the extension of polymer chain in elongation) must be about 5000 to affect the velocity field of the polymer solution. Drag-reduction and pitot tube experiments are unlikely to contain polymers at such a high volume fraction. Therefore, macroscopic manifestation of polymer-polymer interactions occur at moderate volume fraction in flows which are unstable or contain singularities.

Polymer Degradation

The breaking of polymer chains does not cause any of the phenomena associated with viscoelasticity or drag-reduction, but degradation of the polymer solution must be of concern when conducting drag reduction and solution characterization experiments.

Polymers in elongational flow fields break near the center of the backbone of the polymer which provides strong evidence that the polymers are unraveled during elongational flows (see Odell & Keller 1986 and Merr'll & Horn 1984). Breaking in the center greatly reduces the average molecular weight, and the higher molecular weight polymers break first, so degradation greatly changes the viscoelasticity of polymer solutions. Also, chemical degradation can ruin polymer solutions. For example, the polyethylene oxide back-bone is attacked by both ferric ions and chlorine (see Hoyt 1980).

Summary

At this juncture it is worthwhile restating the important points made in this section. The rheological property most likely to be responsible for the drag reducing characterisitics of dilute polymer solutions (elongational viscosity) is the most diffficult to measure. In fact, except for the viscosity of non-Newtonian fluids, attempts to provide the correct values of rheological properties for a predictive model have been unsuccessful or of limited value.

Finally, recommendations for future directions have been made. First, an research approach must be adopted which examines flows which contain a mixture of shear and elongation (e.g. Dunlap and Leal). Further, simultaneous numerical simulation and experimental investigations is the only way to determine the efficacy of candidate constitutive equations to predict changes in turbulence due to polymers.

Transient Viscoelastic Stresses In Turbulent Flows

The goal of our research is to predict modification of turbulence caused by viscoelastic fluids. Currently, the calculation of Newtonian turbulent flow taxes the available computing power of even the fastest and largest supercomputers. We need to gain as much information as we can from the Newtonian simulations with regard to the mechanisms by which viscoelastic fluids may respond to turbulent deformations before attempting the simulation of viscoelastic turbulent flow.

The short term objective is to calculate viscoelastic stresses which exist in a turbulent flow, if the viscoelastic fluid does not alter the Newtonian kinematics. With this assumption, the viscoelastic stresses can then be calculated from the Newtonian kinematics which can be obtained from the Naval Research Laboratory's turbulent channel flow simulations.

First, we discuss the motivation for this research – combining studies of previous drag reducing theories, non-Newtonian properties, and rheology of fluid models. Next, we quantify the kinematics necessary for non-Newtonian behavior, especially the enhancement of the elongational viscosity, and quantify the kinematics found in the direct Newtonian simulations. Then, we present an approximate method to calculate the stresses from the turbulence kinematics. Finally, we show kinematics from the new de-aliased simulations, and discuss the conclusions.

Previous Drag Reduction Theories

Many drag reduction theories only correlate the Reynolds number at which drag reduction begins to occur with a single characteristic of the viscoelastic fluid: for example, the length and time scale correlations. Other theories are phenomenological models based on a single property of a viscoelastic fluid: such as the relative reduction in stress as the oscillatory frequency is increased or the finite rise time of viscoelastic stresses.

No existing theory can predict the modifications of turbulence which occur due to the viscoelasticity of the fluid. For example, the fluctuations in the streamwise component of the velocity increases in the buffer region of turbulent viscoelastic flows (compared to Newtonian flows), while the spanwise component decreases. A more complete theory or analysis is required to begin to understand these important changes in the structure of the turbulence.

Current Approach

We examine four characteristics of viscoelastic stresses. First, normal stresses are those which develop normal to the shear stress. Second are the time-dependent stresses due to the finite response time of stresses. Third, rate-dependent viscometric functions exist because stress levels are not linearly related to the rates of deformations. Lastly, elongational viscosities exist because the resistances to elongational deformations are orders of magnitude larger than for Newtonian fluids.

We use Newtonian kinematics from the Newtonian turbulence simulations to quantify the importance of the four characteristics listed above. These kinematics, which involve spatial gradients in a rapidly fluctuating velocity field, are not measurable with current experimental techniques.

Viscometric Flows

For a Newtonian fluid in shear flow, the stress tensor contains only two non-zero elements. A viscoelastic fluid on the other hand develops "normal" stresses besides the two off-diagonal components. The viscosity of a viscoelastic fluid is a function of both the shear rate and the duration of the shearing, instead of being a constant, as with Newtonian fluids. The normal stress coefficients are also functions of the shear rate and time, whereas these normal stress coefficients are zero in Newtonian fluids.

In pure elongational flows, a spatial velocity gradient exists in the direction of velocity. In this deformation field, both Newtonian and viscoelastic fluids develop

stresses only along the diagonal of the stress tensor. However, the relative magnitudes of these stresses in a viscoelastic fluid can be much larger than for Newtonian fluids. The elongational viscosity is defined as the difference between the first two diagonal components divided by the elongation rate. The elongational viscosity of a Newtonian fluid is three, while the value for a viscoelastic fluid is a function of elongation rate and the duration of the elongation. Note that the "normal" stresses from shear flows alter the elongational viscosity by altering the diagonal stresses.

Time Scales

The relaxation time of a viscoelastic fluid is the time constant for the relaxation of stresses in the fluid upon cessation of deformations. This relaxation time is also the rate at which stresses rise to their steady values upon the imposition of deformations.

The retardation time represents the solvent contribution to the stresses in shear flows at vanishingly small deformations. It is defined as the ratio of the solvent to the viscoelastic fluid viscosities (at small deformations) times the relaxation time of the viscoelastic fluid. In dilute polymer solutions, the ratio of viscosities is almost unity, so the ratio of the retardation time to the relaxation time is also near unity.

Molecular Models and Constitutive Equations

The Maxwell molecular model represents two beads connected by a spring in series with a dashpot. The relaxation time is equal to the ratio of the viscosity of the dashpot to the modulus of the spring. To incorporate a solvent viscosity into the model, one can add a dashpot in parallel with the dashpot/spring elements. This model is called the Oldroyd-B model (see Bird *et al.*1987a). In order to more closely match viscoelastic fluids, other modifications can be incorporated into a fluid model. Any constitutive equation can be analyzed with the technique applied below. The Oldroyd-B model is chosen because it contains the basic features of most continuum models.

Kinematics Which Lead to Non-Newtonian Behavi r

The type of deformation a viscoelastic fluid undergoes is the prime factor in determining whether the fluid shows a marked deviation from Newtonian behavior. In shear flows, fluid elements separate linearly with respect to time; whereas, in elongational deformations fluid elements separate exponentially in time. Therefore, even transient elongational deformations produce non-Newtonian behavior.

The second factor is the strength of the shear or elongational deformation. At low flow strengths (with respect to the relaxation time of the viscoelastic fluid) the stresses in the fluid and the flow itself are close to Newtonian. Above certain elongation rates, infinite stresses are predicted to exist in the flow of some fluid models. It is critical to know if these limiting rates are exceeded for long periods of time.

Another factor is the duration of the deformations. Polymers require a finite period of time to deform. Short duration deformations only generate a Newtonian response from the viscoelastic fluid. The viscoelastic contributions to the overall stress levels in a fluid element rise at a rate proportional to the relaxation time of the viscoelastic fluid. For these contributions to affect the flow, the deformations must remain large for a finite period of time.

Finally, it is crucial to determine the relative strength of the steady shear with respect to the elongational components of the deformations. If the normal stresses which develop due to the shearing are to alter the elongational stresses appreciably, and hence modify the flow, then the ratio of the mean shear to the magnitude of the fluctuating elongation must be greater than one.

Strain Rate and Vorticity

An overall measure of the strength of a flow is to compare the magnitude of the strain rate, defined as the symmetric portion of the gradient of the velocity, to the vorticity, defined as the anti-symmetric portion of the velocity gradient. These data at

one point from the numerical simulations are plotted in Figure 10. The calculations were at a Reynolds number of 3900, based on channel half-width and centerline velocity. The point is at a distance of 16 viscous units away from the wall. A viscous unit is the ratio of the kinematic viscosity over the shear velocity. In regions in which the strain rate is greater than the vorticity, the molecule undergoes deformations. Otherwise the molecules are rotating too rapidly to develop a large aspect ratio. These kinematics cannot currently be obtained from experiments, but this type of information is easily extracted from direct simulations.

Extensional Flow of Oldroyd-B Model With Imposed Shear

It is crucial to examine the time-dependent nature of these models. The transient elongational viscosity of the Oldroyd-B model is shown as the lower curve in Figure 11. The elongational viscosities begin at three times the retardation time (set to 2/3 for this and all other calculations presented below) and rise to their steady-state value only after about ten relaxation times have elapsed.

Now we can look at the effect of the presence of a mean shear on the elongational viscosity (stresses). Steady shear is imposed on the fluid at a dimensionless value of 1.0. while the transient elongation rate remains at 0.40. These data are the upper curve of Figure 11. The enhancement of the elongational viscosity remains about constant with time with respect to the no shear case. The elongational viscosity is approximately doubled.

The steady elongational viscosity of the Oldroyd-B model is shown in Figure 12 as the lower curve. The elongational viscosities of viscoelastic models are quite different and bear no resemblance to the constant Newtonian elongational viscosity of three at all elongation rates. The Oldroyd-B model has a elongational viscosity of three at low elongation rates, and then the elongational viscosity rises to infinity at a dimensionless elongational rate of one-half. All evidence indicates that the elongational viscosities of viscoelastic fluids rise well above the Newtonian value (one to three orders of magnitude).

The steady elongational viscosity of the Oldroyd-B model with an imposed shear is shown as the upper curve on Figure 12. The enhancement of the elongational viscosity due to a mean shear is larger at low values of the elongation rate. The stresses produced by the shearing are constant, so the enhancement of the elongational viscosity (which is the ratio of stress to elongation rate) decreases as the elongation rate increases. Therefore, enhancement of the elongational viscosity damps out small elongations more severely than large elongations. This asymmetry agrees with the results which we have found experimentally in the pressure spectra of turbulent drag-reducing solutions. The higher frequencies are attenuated to a much greater extent than the lower frequencies.

Deformation Rates As a Function of Position In the Channel

Now let us look at the kinematics of turbulent flow. We have direct simulations of turbulent Newtonian channel flow at a Reynolds number of 3900. A plot of the mean and fluctuating shear rate as a function of channel position in wall units is shown in Figure 13. These results were obtained by assuming a 2.54 cm channel height and water as the fluid. The buffer region of the channel is located between the dotted lines. The mean shear rate is small above the buffer region. The data in the figures presented below are for points at a distance from the wall of 16 viscous units – the location of the dashedline on Figures 13 and 14.

The root-mean-square (RMS) of the three elongational components as a function of position in the channel are presented in Figure 14. The streamwise component of elongation is the 11-term, the wall-normal is the 22-term, and the spanwise is the 33-term. All three functions peak in the buffer region. These RMS values do not indicate the distribution of the deformations. The peak values range from 7 to 12 s^{-1}. These elongation rates are not measurable in experiments: they are spatial gradients of velocity in a fluctuating velocity field. Presently, only through simulation of turbulent flow can these deformations be quantified.

Probability Density Function of the Streamwise Elongation Rate

The probability density function for the streamwise component of the elongation at a wall-normal position of 16 viscous units is shown on Figure 15 (solid squares and solid line). A normal distribution with the same mean and standard deviation is also shown for comparison (hollow circles and dashed line). The distribution is not a normal distribution; the center is more peaked and there is more probability density in the tails.

Power Spectral Density of the Streamwise Elongation Rate

The frequencies of the elongational deformations are also critical in determining the change in the stress tensor. The power spectral density of the streamwise deformation component as a function of frequency is presented in Figure 16. The density contains a peak at 10 Hz, therefore it is the most common frequency for that deformation.

Energy Dissipation in Oscillating Flow Field

The average values of the steady shear, oscillating shear, oscillating elongations, and frequency found from the data just presented can now be used to evaluate the energy dissipation which occurs with sinusoidal deformations (Figure 17). The ratios of the various deformations are maintained as constant, while the values of the deformations are increased. The ratio of the energy dissipation for a fluid model to the dissipation for a Newtonian fluid is plotted as a function of the strength of the deformations. Note that with either a retardation time or a mean shear, the reduction in energy dissipation is minimal. In fact, if a retardation time and a mean shear are included, then the energy dissipation is reduced only one percent. Oscillating shear alone does not seem to be a feasible mechanism for drag reduction. The mean shear is lower in the central portion of the flow, but the amplitude of the oscillating shear is also lower. Most of the turbulent energy is near the walls, where the mean shear rate is significant.

Stresses During Sinusoidal Deformations

To determine the response of a viscoelastic fluid to the various deformations that have been now quantified, the stresses of the viscoelastic fluid are calculated as a function of time in a homogeneous flow field of sinusoidal elongation and steady shear. The mean shear is assumed to be 100 s^{-1}, the amplitudes of the shear and elongation are 47 and 8.5 s^{-1}, respectively, the frequency of the oscillation is 10 Hz, and the relaxation time of the viscoelastic fluid is 10 msec. Estimates in the literature range from 3 to 50 msec. At this frequency, the shear stress is very close to the Newtonian stress (see Figure 18).

In the case of the normal stress, the stress levels become asymmetric due to the steady and oscillating shear, as shown on Figure 19. The "normal" stresses from the shearing contribute the same amount of stress to both phases of the oscillating deformation, so the stress is reduced during compression of the fluid element and increased during elongation. Also, the amplitude of the oscillations are not damped, as would be the case with no shear. The kinematics are altered by this asymmetry.

Deformation Rates

Recently, we have determined that our channel flow simulations of Newtonian turbulence contained errors in comparison with experimental results. The errors in the simulations are due to aliasing. The calculation of non-linear terms are producing excess energies at some of the wavenumbers in the spectral decomposition of the problem. More recent simulations with de-aliasing have not been calculated up to the Reynolds number of the older simulations, from which the kinematics presented above are extracted. At the lower Reynolds number of 2130, the steady and oscillating values of the shear rate across the channel are reported in Figure 20. The mean shear in the buffer layer is now about 34 s^{-1}, instead of 100 s^{-1}. The oscillating component is about 22, instead of 47.

The elongation rates are reduced even more, as can be seen in Figure 21. The RMS value of the streamwise component is 2.2, instead of 6. The shapes of the curves

are smoother and the maximums occur at the same y-location, which may be due to the lower Reynolds number or the de-aliasing.

Viscoelastic Stresses in Turbulent Flow

We have integrated the stresses of the Oldroyd-B model as a function of time, obtaining the deformations from the Newtonian turbulence simulations at a Reynolds number of 2130. To obtain these results, we substitute the spatial gradient of the deformation rate in place of the spatial gradient of the stress, which appears in the convected derivative. These gradients are equal for Newtonian fluids. This approximation allows the highly convective and non-homogeneous nature of the turbulent flow to be modelled without knowing the viscoelastic stress distribution for the entire flow field. The shear stress and the streamwise normal stress are plotted in Figure 22. Because of the method used to non-dimensionalize the stresses, the Newtonian stresses are equal to the negative of the deformation rate for the same component. Differences between the Newtonian and the Oldroyd-B stresses do occur, principally in the form of a delay between the deformation and the stress level. Much greater differences are found if the relaxation time of the fluid is assumed to be 50 ms, instead of 10 ms. These results are shown in Figure 23. For this relaxation time, large excursions occur in the elongational stress due to changes in the shear rate, and the delay between stress and strain is several relaxation times (easiest seen by examining the shear deformation and stress curves). We expect these large differences to occur for fluids with lower relaxation times, but at higher Reynolds numbers.

Conclusions

The "normal" stresses generated by the mean shearing which occur in the buffer region are significant contributors to the stress levels. The ratio of mean shear to RMS elongation is about 10.

The magnitudes of the shear and elongational deformations and the duration of the deformations are important in selecting a constitutive equation and in determining

which aspects of viscoelasticity modify turbulent flow and reduce drag. These findings are obtained from a low Reynolds number simulation, at about half the Reynolds number at which drag reduction can be accurately measured with an aqueous solution (60 ppm) of polyethylene oxide solution in the channel flow facility at NRL (2.54 cm channel height). The findings discussed below probably apply in a turbulent flow at double the calculated Reynolds number, but probably only the effect of "normal" stresses remain at high Reynolds numbers. First, the product of twice the elongation rate and the relaxation time is less than unity. Second, the duration of the elongations (about 20 ms) are longer than the assumed relaxation time of the fluid (10 ms), but shorter than some estimates (50 ms). The durations are not, however, on the order of one hundred relaxation times, which implies elongational stresses do not reach their steady-state values at high elongation rates.

The critical parameter, as seen in the above analysis, is the relaxation time of the viscoelastic fluid. Knowledge of this time constant is crucial in determining the regimes in which the flow exists with regard to deviations from Newtonian behavior. The retardation time (or more precisely, the ratio of retardation to relaxation times) is also an important parameter. The retardation time acts to dampen non-Newtonian behavior, especially in that the retardation time decreases the "normal" stresses produced by shearing.

References

Bagley, E.B. 1957 End correction in the capillary flow of polyethylene. *J.Appl.Phys.* **28**, 624-627.

Baid, K.M. & Metzner, A.B. 1977 Rheological properties of dilute polymer solutions determined in extensional and shearing experiments. *Trans.Soc.Rheol.* **21**, 237-260.

Balakirshnan, C. & Gordon, R.J. 1971 New viscoelastic phenomenon and turbulent drag reduction. *Nature* **231**, 177-178.

Beard, D.W., Davies, M.H. & Walters, K. 1966 The stability of elastico-viscous flow between rotating cylinders. Part 3. Overstability in viscous and Maxwell fluids. *J.Fluid Mech.* **24**, 321-334.

Becraft, M.L. & Metzner, A.B. 1988 Bourdon tube effects in the fiber spinning apparatus. *J.Rheol.* **32**, 243-270.

Belokon, V.S., Kalashnikov, V.N, Kudin, A.M. & Vlasov, S.A. 1973 Rheological properties of polymers reducing drag friction. *Prog.Heat Mass Trans.* **5**, 233-237.

Berman, N.S. 1978 Drag reduction by polymers. *Ann.Rev.Fluid Mech.* **10**, 47-64.

Bird, R.B., Armstrong, R.C., & Hassager, O. 1987a *Dynamics of Polymeric Liquids. 2nd Ed., Vol.1: Fluid Mechanics.* Wiley, New York. 647 p.

Bird, R.B., Curtiss, C.F., Armstrong, R.C., & Hassager, O. 1987b *Dynamics of Polymeric Liquids, 2nd Ed., Vol.2: Kinetic Theory.* Wiley, New York. 437 p.

Brodnyan, J.G., Gaskins, F.H. & Philippoff, W. 1957 On normal stresses, flow curves, flow birefringence, and normal stresses of polyisobutylene solutions. Part II. Experimental. *Trans.Soc.Rheol.* **1**, 109-118.

Chakraborty, A.K. & Metzner, A.B. 1986 Sink flows of viscoelastic fluids. *J.Rheol.* **30**, 29-41.

Chang, C. & Schowalter, W.R. 1974 Flow near an oscillating cylinder in dilute viscoelastic fluid. *Nature* **252** 686-688. & Errata. 1975 *Nature* **253**, 572.

Chang, C. & Schowalter, W.R. 1979 Secondary flow in the neighborhood of a cylinder oscillating in a viscoelastic fluid. *J.N.-N.Fluid Mech.* **6**, 47-67.

Chiou, C.S. & Gordon, R.J. 1976 Vortex inhibition: Velocity profile measurements. *AIChE J.* **22**, 947-950.

Crowley, D.G., Frank, F.C., Mackley, M.R & Stephenson, R.G. 1976 Localized flow birefringence of polyethylene oxide solutions in a four roll mill. *J.Poly.Sci.:Poly.Phys.Ed.* **14**, 1111-1119.

Dandridge, A., Meeten, G.H., Layec-Raphalen, M.N. & Wolff, C. 1979 Flow birefringence of dilute solutions of polyethyleneoxide of high molecular weight at high rates. *Rheol.Acta* **18**, 275-279.

Darby, R. & Chang, H.D. 1984 Generalized correlation for friction loss in drag reducing polymer solutions. *AIChE J.* **30**, 274-280.

DeGennes, P.G. 1974 Coil-stretch transition of dilute flexible polymers under ultrahigh velocity gradients. *J.Chem.Phys.* **60**, 5030-5042.

Denn, M.M. & Roisman, J.J. 1969 Rotational stability and measurement of normal stress functions in dilute polymer solutions. *AIChE J.* **15**, 454-459.

Denn, M.M., Sun, Z.-S. & Rushton, B.D. 1971 Torque reduction in finite amplitude secondary flows of dilute polymer solutions. *Trans.Soc.Rheol.* **15**, 415-431.

Deutsch, S. & Phillips, W.M. 1977 The use of the Taylor-Couette stability problem to validate a constitutive equation for blood. *Biorheol.* **14**, 253-266.

Dunlap, P.N. and Leal, L.G. 1987 Dilute polystyrene solutions in extensional flows: birefringence and flow modification. *J.N.-N.Fluid Mech.* **23**, 5-48.

Farrell, C.J., Keller, A., Miles, M.J. & Pope, D.P. 1980 Conformational relaxation time in polymer solutions by elongational flow experiments: 1. Determination of extensional relaxation time and its molecular weight dependence. *Polymer* **21**, 1292-1294.

Fruman, D.H. & Barigah, M. 1982 Rheological interpretation of pressure anomalies of aqueous dilute polymer solutions (ADPS) in orifice flow. *Rheol.Acta* **21**, 556-560.

Fuller, G.G. & Leal, L.G. 1980 Flow birefringence of dilute solutions in two-dimensional flows. *Rheol.Acta* **19**, 580-600.

Gardner, K., Pike, E.R., Miles, M.J., Keller, A., & Tanaka, K. 1982 Photon-correlation velocimetry of polystyrene in extensional flow fields. *Polymer* **23**, 1435-1442.

Ginn, R.F. & Denn, M.M. 1969 Rotational stability in viscoelastic liquids: Theory. *AIChE J.* **15**, 450-454.

Gollub, J.P. & Swinney, M.L. 1975 Onset of turbulence in a rotating fluid. *Phys.Rev.Lett.* **35**, 927-930.

Gordon, R.J. & Balakirshnan, C. 1972 Vortex inhibition: a new viscoelastic effect with importance in drag reduction and polymer characterization. *J.Appl.Poly.Sci.* **16**. 1629-1639.

Hikmet, R.A.M., Narh, K.A., Barham, P.J. & Keller, A. 1985 Adsorption- entanglement layers in flowing high-molecular weight polymer solutions. *Prog.Coll.Poly.Sci.* **71**, 32-43.

Hoyt, J.W. & Fabula, A.G. 1964 The effect of additives on fluid friction. *5th Symposium on Naval Hydrodynamics*, Bergen, Norway, ONR ACR-112, 947-974.

Hoyt, J.W. 1971 Drag-reduction effectiveness of polymer solutions in the turbulent-flow rheometer: a catalog. *Poly.Lett.* **9**, 851-862.

Hoyt, J.W. 1972 The effects of additives in fluid friction. *Trans.ASME:J.Basic Engg.* **94**, 258-285.

Hoyt, J.W. 1980 Effect of ferric ions on drag reduction effectiveness of polyacrylamide. *Poly.Sci.Engg.* **20** , 493-498.

James, D.F., McLean, B.D. & Saringer, J.H. 1987 Presheared extensional flow of dilute polymer solutions. *J.Rheol.* **31**, 453-481.

James, D.F. & Saringer, J.H. 1982 Flow of dilute polymer solutions through converging channels. *J.N.-N.Fluid Mech.* **11**, 317-339.

Jones, W.M., Davies, D.M., & Thomas, M.C. 1973 Taylor vortices and the evaluation of material constants: a critical assessment. *J.Fluid Mech.* **60**, 19-41.

Keller, A. & Odell, J.A. 1985 The extensibility of macromolecules in solution: a new focus for macromolecular science. *Coll.Poly.Sci.* **263** , 181-201.

Kowalik, R.M., Duvdevani, I., Peiffer, D.G., Lundberg, R.D., Kitano, K. & Schulz, D.N. 1987 Enhanced drag reduction via interpolymer associations. *J.N.-N.Fluid Mech.* **24**, 1-10.

Larson, R. 1988 *Constitutive Equations for Polymer Melts and Solutions.* Butterworth, Stoneham, Massachusetts. 304 p.

Lawler, J.V. 1986 Laser-Doppler velocimetry of viscoelastic flow between eccentric rotating cylinders. Ph.D. Thesis. MIT, Cambridge, Massachusetts.

Lawler, J.V., Handler, R.A. Hendricks, E.W. & Leighton, R.I. 1987 Transient normal stresses in turbulent flows. Paper F5. *59th Ann.Meet.Soc.Rheol.*, Atlanta, Georgia (publication in preparation).

Little, R.C., Hansen, R.J., Hunston, D.L., Kim, O., Patterson, R.L. & Ting, R.Y. 1975 The drag-reduction phenomenon. Observed characteristics, improved agents, and proposed mechanisms. *Ind.Eng.Chem.Fund.* **14**, 283-296.

Lodge, A.S. 1955 Variation of flow birefringence with stress. *Nature* **176**, 838-839.

Lumley, J.L. 1969 Drag reduction by additives. *Ann.Rev.Fluid Mech.* **1**, 367.

Lumley, J.L. 1973 Drag reduction in turbulent flow by polymer additives. *J.Polym.Sci:Macromol.Rev.* **7**, 263-290.

Matthys, E.F. 1987 Laser-induced photochromic flow visualization: measurement of velocities and deformation rates. Paper E14. *59th Annual Meeting of the Society of Rheology,* Atlanta, Georgia, October 1987.

Merrill, E.W. & Horn, A.F. 1984 Scission of macromolecules in dilute solution: Extensional and turbulent flows. *Poly.Comm.* **25**, 144-146.

Metzner, A.B., & Astarita, G. 1967 External flow of viscoelastic materials: fluid property restrictions on the use of velocity-sensitive probes. *AlChE J.* **13**, 550-555.

Odell, J.A. & Keller, A. 1986 Flow-induced chain fracture of isolated linear macromolecules in solution. *J.Poly.Sci.:Poly.Phys.Ed.*, **24** , 1889-1916.

Odell, J.A., Keller, A. & Miles, M.J. 1985 Assessment of molecular connectiveness in semi-dilute polymer solutions by elongational flow. *Polymer* **26**, 1219-1226.

Olbricht, W.L., Rallison, J.M. & Leal, L.G. 1982 Strong flow criteria based on microstructure deformation. *J.N.-N.Fluid Mech.* **10**, 291-318.

Phan-Thien, N., Manero, O., & Leal, L.G. 1984 A study of conformation-dependent friction in a dumbbell model for dilute solutions. *Rheol.Acta* **23**, 151-162.

Philippoff, W. 1956 Flow-birefringence and stress. *Nature* **178** , 811-812.

Ryskin, G. 1987a Turbulent drag reduction by polymers: A quantitative theory. *Phys.Rev.Lett.* **59**, 2059-2062.

Ryskin, G. 1987b Calculation of the effect of polymer additive in a converging flow. *J.Fluid Mech.* **178**, 423-440.

Sun, Z. & Denn, M.M. 1972 Stability of rotational Couette flow of polymer solutions. *AIChE J.* **18**, 1010-1015.

Tanner, R.I. 1985 *Engineering Rheology.* Oxford University, New York. 451 p.

Taylor, G.I. 1923 Stability of a viscous liquid contained between two rotating cylinders. *Phil.Trans.Roy.Soc.London A* **223**, 289-343.

Ting, R.Y. & Hunston, D.L. 1977 Polymeric additives as flow regulators. *Ind.Eng.Chem.Prod.Res.Dev.* **16**, 129-136.

Toms, B.A. 1948 Some observations on the flow of linear polymer solutions through straight tubes at large Reynolds numbers. *Proc.1stIntl.Congr.Rheol.* **2**, 135-141.

Usui, H. & Sano, Y. 1981 Elongational flow of dilute drag reducing fluids in a falling jet. *Phys.Fluids* **24**, 214-219.

Virk, P.S. 1975 Drag reduction fundamentals. *AIChE J.* **21**, 625-656.

Vlassopoulos, D. & Schowalter, W.R. 1988 Private communication.

Weinberger, C.B. & Goddard, J.D. 1974 Extensional flow behavior of polymer solutions and particle suspensions in a spinning motion. *Intl.J.Multiphase Flow*, 1, 465-486.

Zimm, B.H. 1956 Dynamics of polymer molecules in dilute solution: viscoelasticity, flow birefringence and dielectric loss. *J.Chem.Phys.* **24**, 269-278.

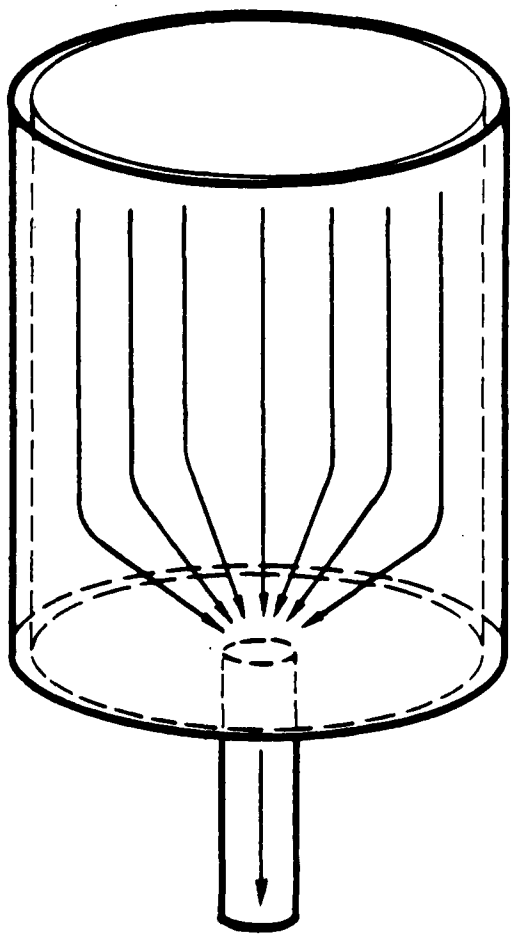

Figure 1. Orifice Flow Geometry

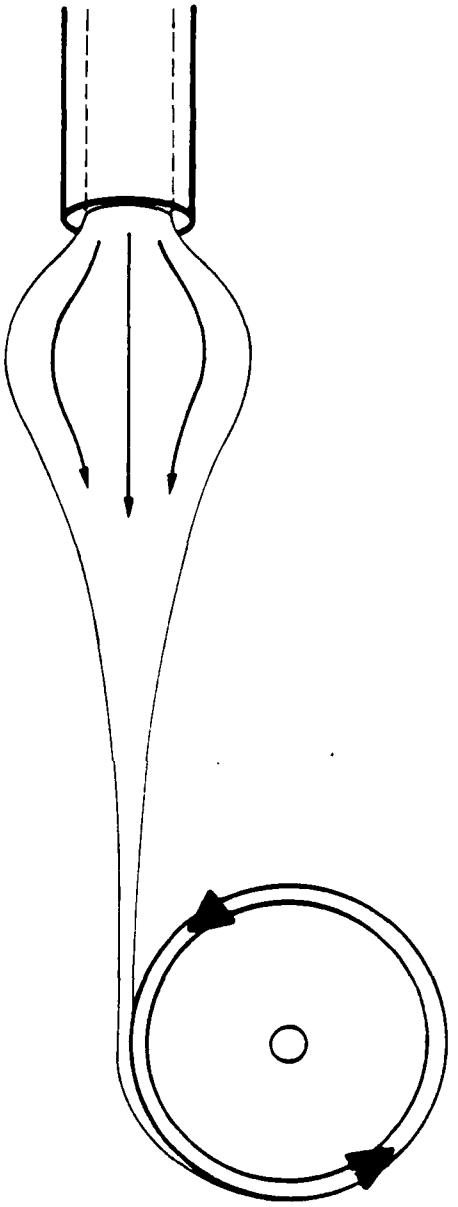

Figure 2. Fiber-Spinning Geometry.

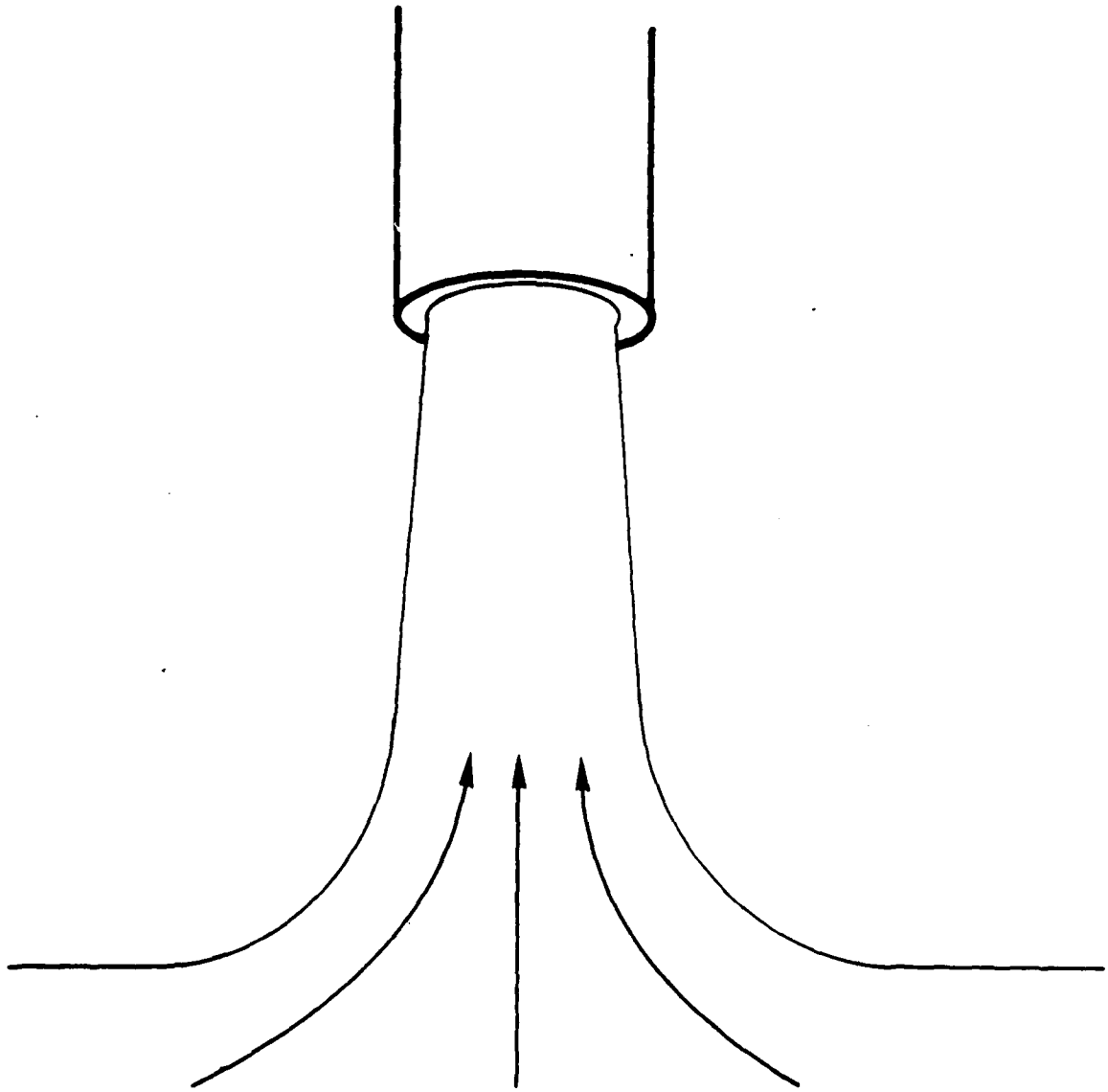

Figure 3. Ductless Syphon Geometry.

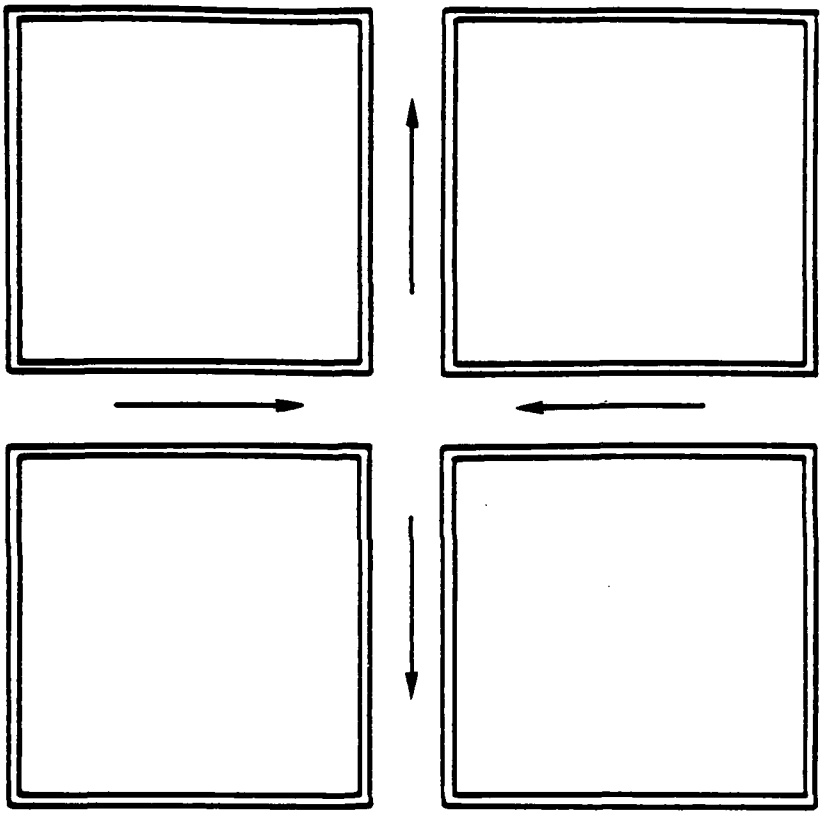

FIgure 4. Crossed-Slots Geometry.

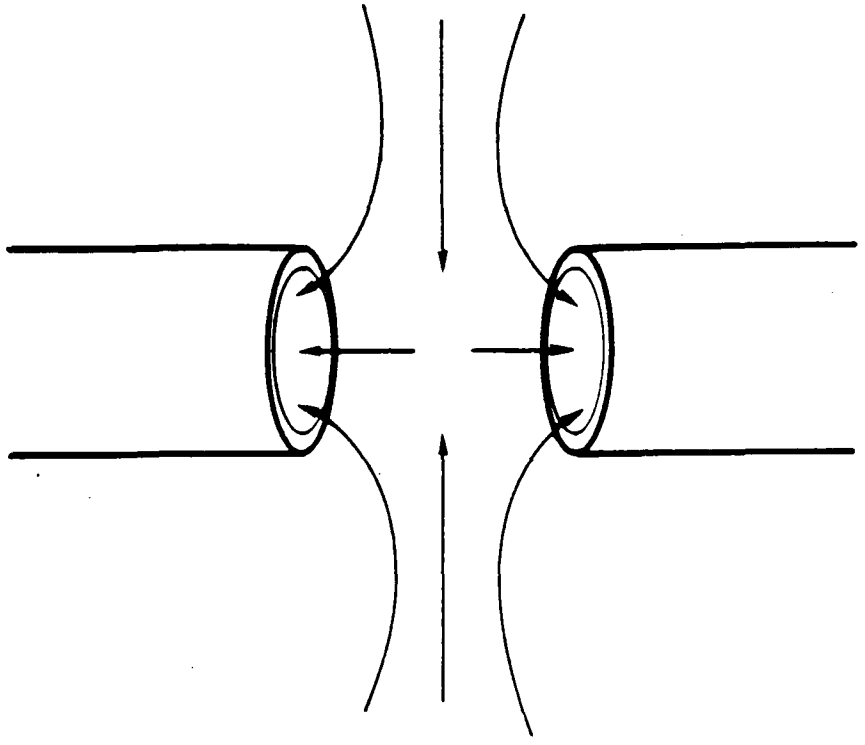

Figure 5. Opposed-Jets Geometry.

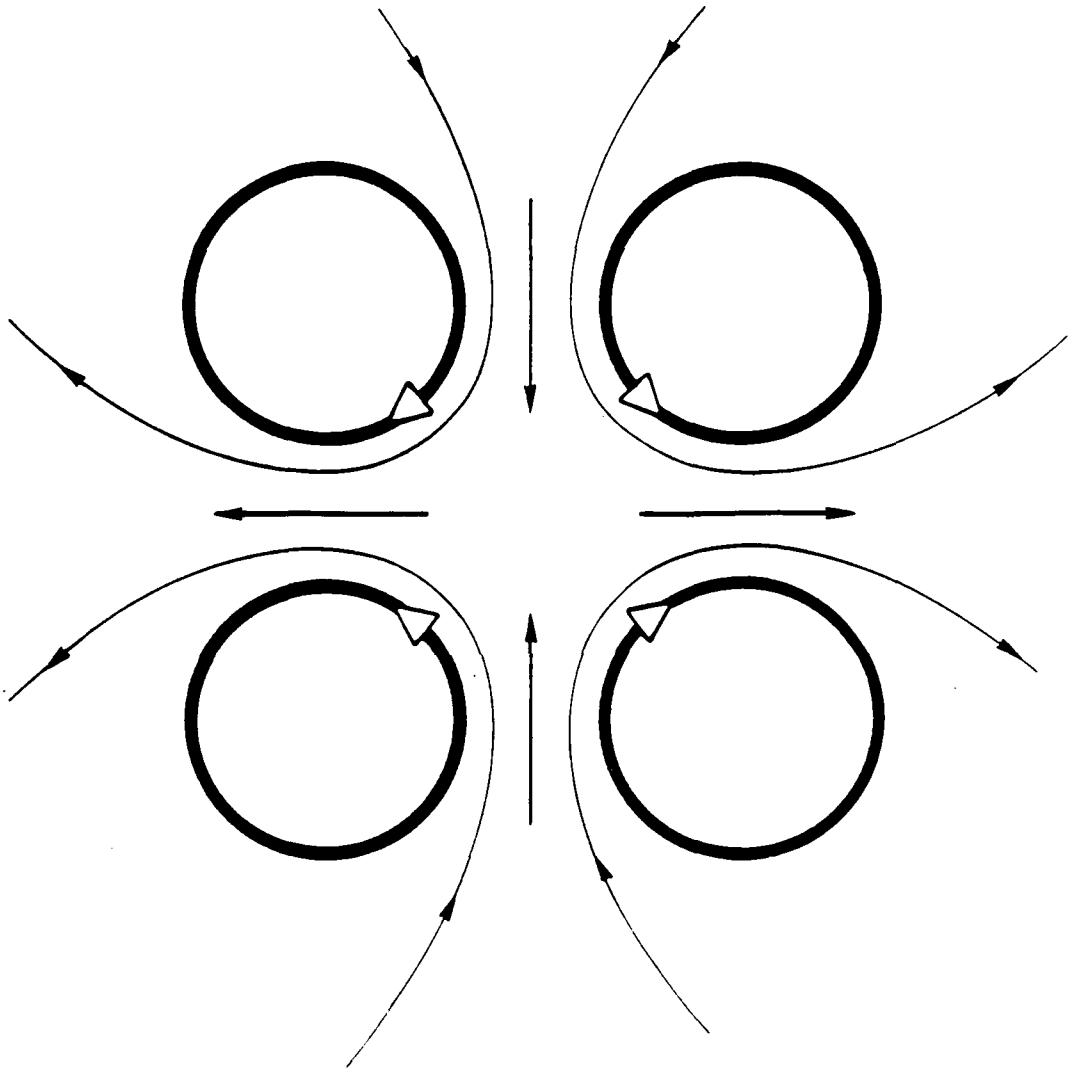

Figure 6. Four-Roll Mill Geometry.

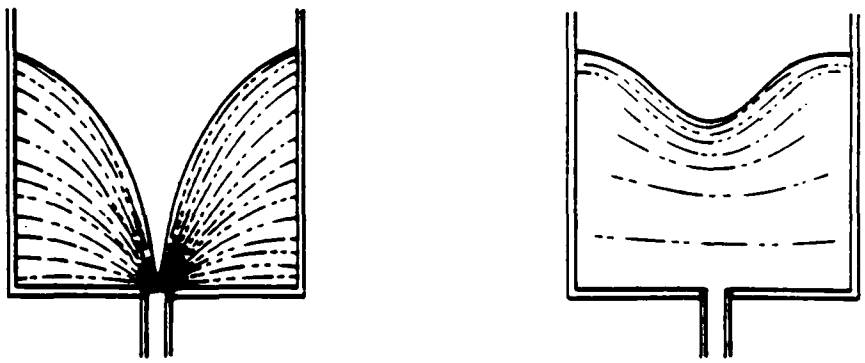

Figure 7. Tank Draining Through An Orifice Geometry.

A) A Newtonian fluid forms a central vortex extending down to the orifice. B) A polymer solution develops a much weaker vortex which does not extend down to the orifice.

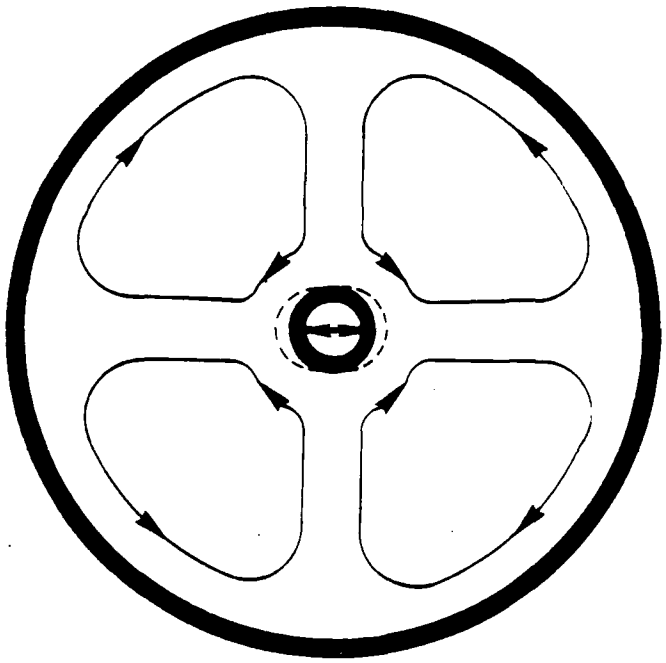

Figure 8. Vibrating Rod Geometry.

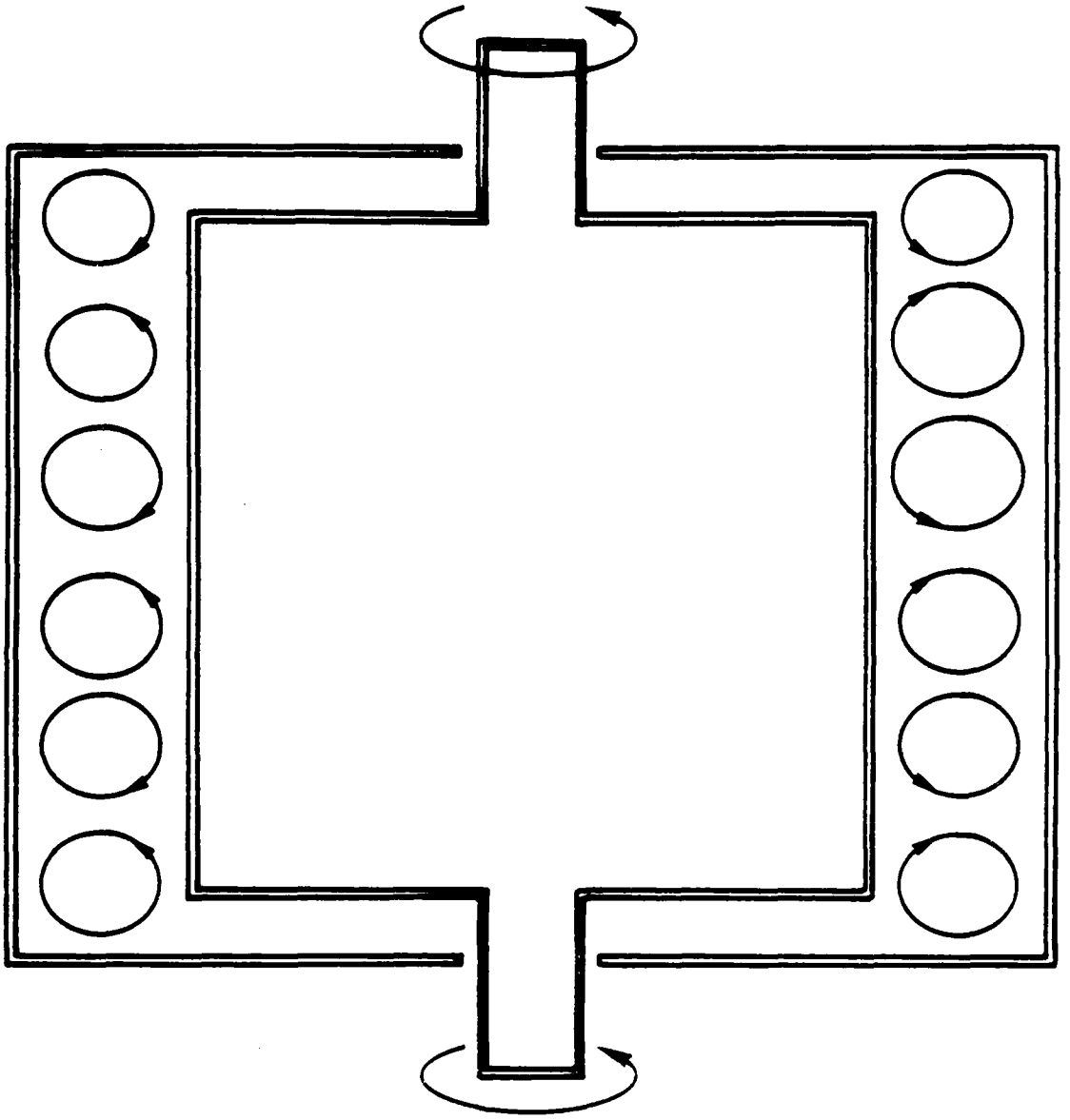

Figure 9. Concentric Cylinder Geometry.

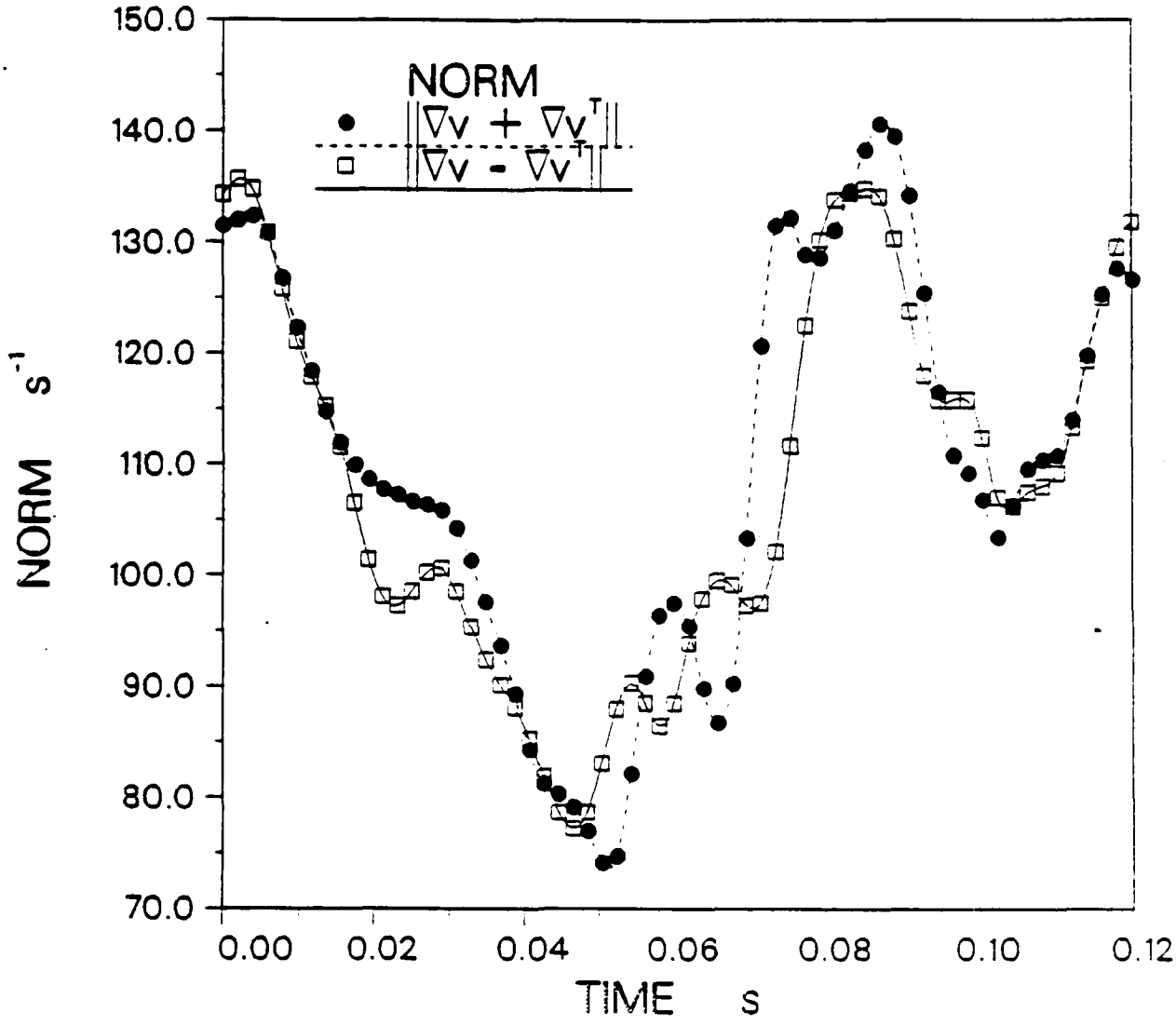

Figure 10. Strain Rate and Vorticity As a Function of Time.

Data from the direct numerical simulations at Re = 3900, at a distance from the wall of 16 viscous units.

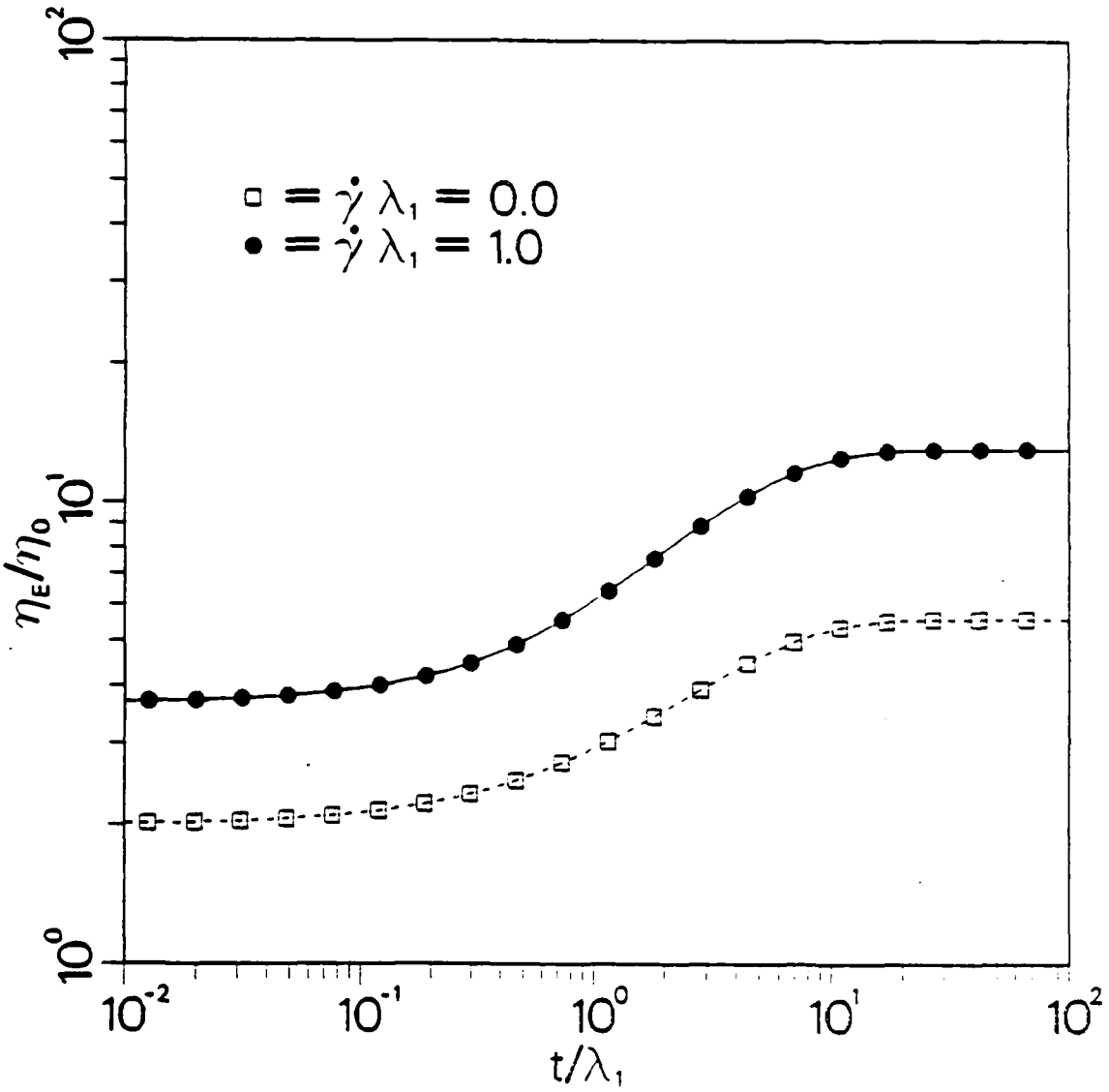

Figure 11. Elongational Viscosity As a Function of Time.

Calculated for Oldroyd-B model with ratio of retardation time to relaxation time of 2/3. The elongation rate times the relaxation time for both curves is 0.4. The elongation begins at time = 0. Viscosity without imposed steady shear is lower curve (hollow squares). Viscosity with imposed steady shear of 1.0 (relaxation time times shear rate) is upper curve (solid circles).

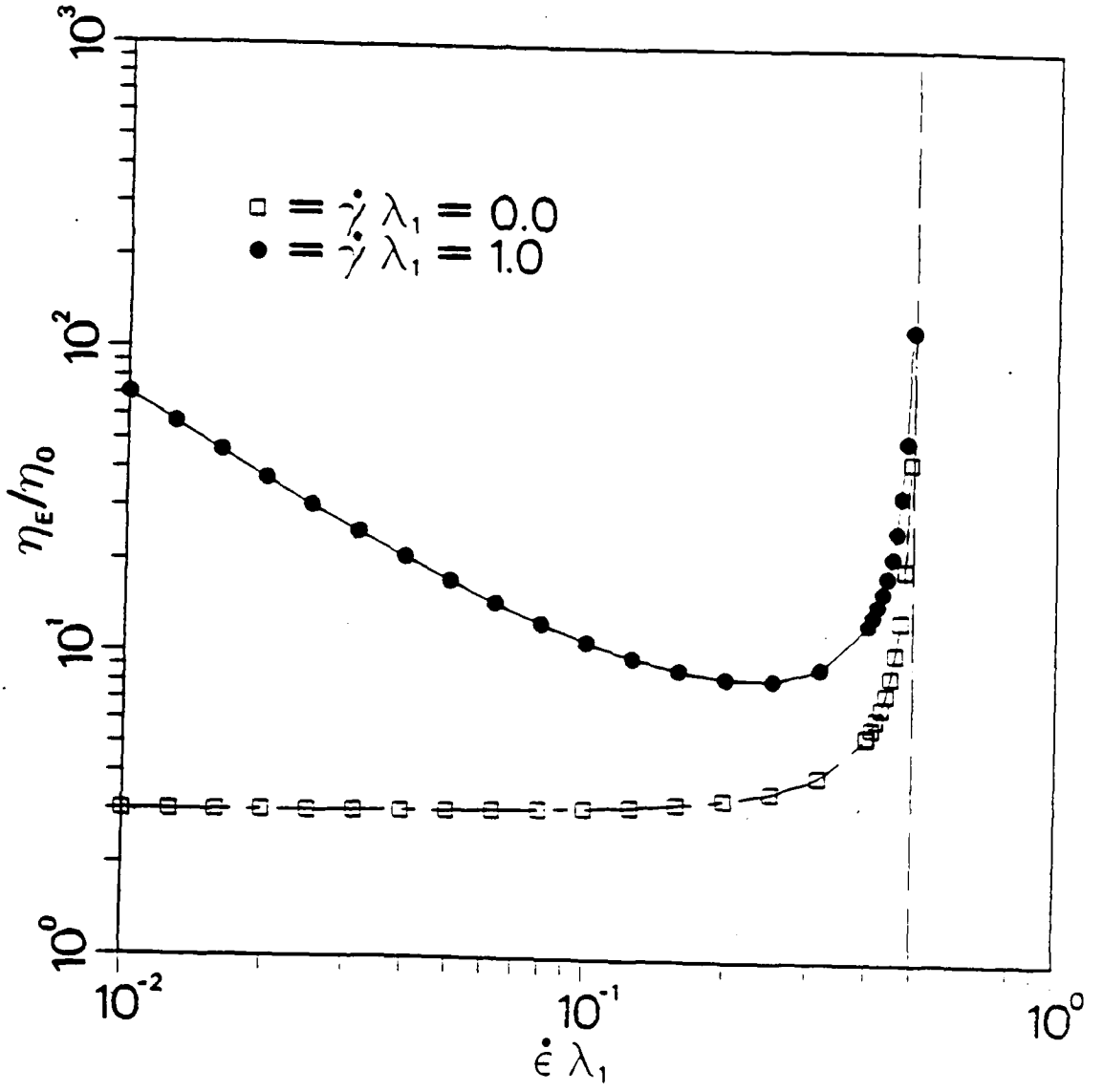

Figure 12. Elongational Viscosity As a Function of Elongation Rate.

Calculated for Oldroyd-B model with ratio of retardation time to relaxation time of 2/3. The elongation has been continued until the stresses have reached steady-state. Viscosity without imposed steady shear is lower curve (hollow squares). Viscosity with imposed steady shear of 1.0 (relaxation time times shear rate) is upper curve (solid circles). Model predicts an infinite viscosity at an elongation rate of 0.5 (dashed vertical line).

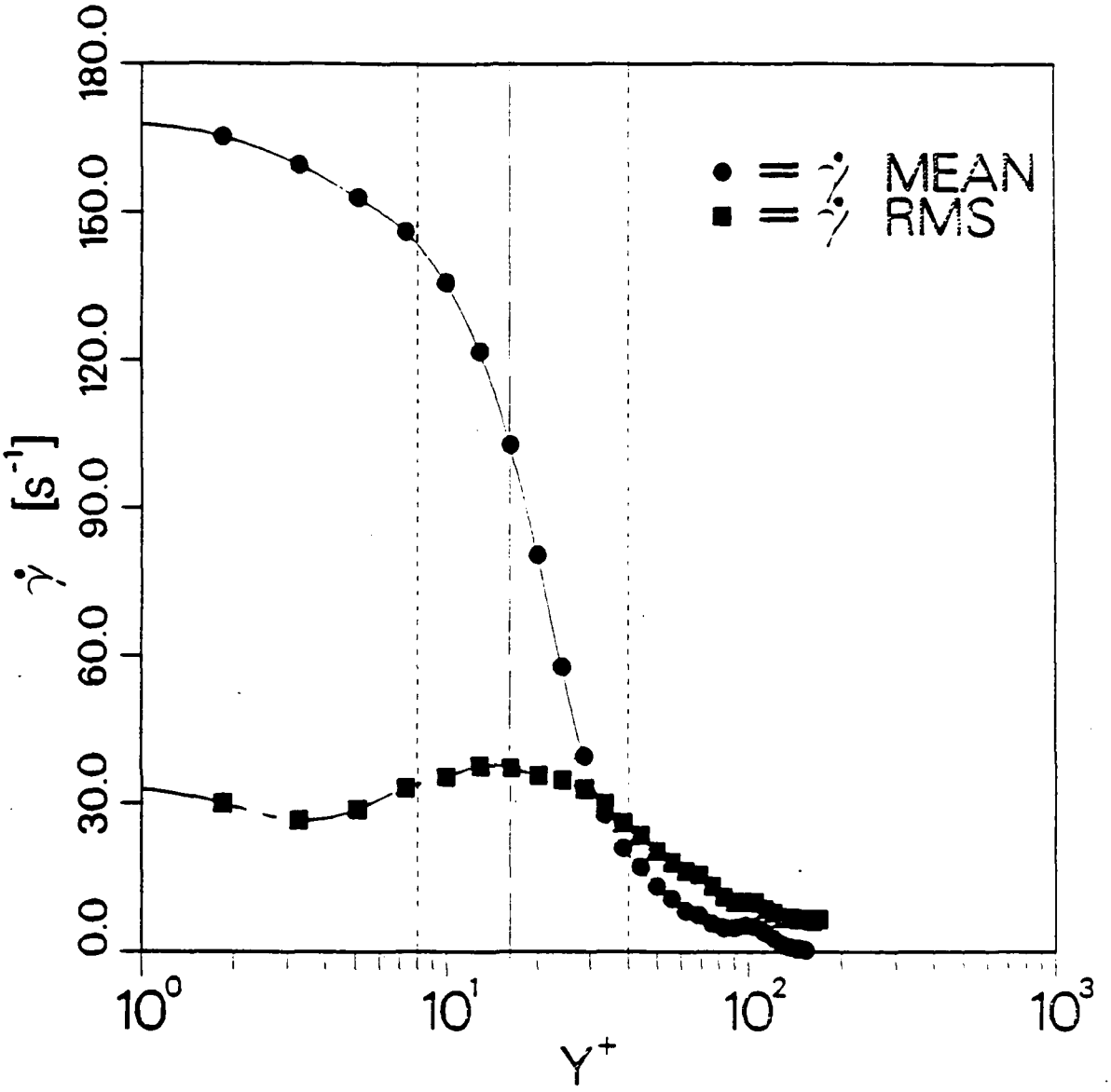

Figure 13. Shear Rate Across a Turbulent Channel.

Mean and root-mean-square shear rate across a channel of infinite planar extent. Results are from a direct numerical simulation of Newtonian flow at Re = 3900. Data is scaled to channel width of 2.54 cm. The buffer region is between the short-dashed lines.

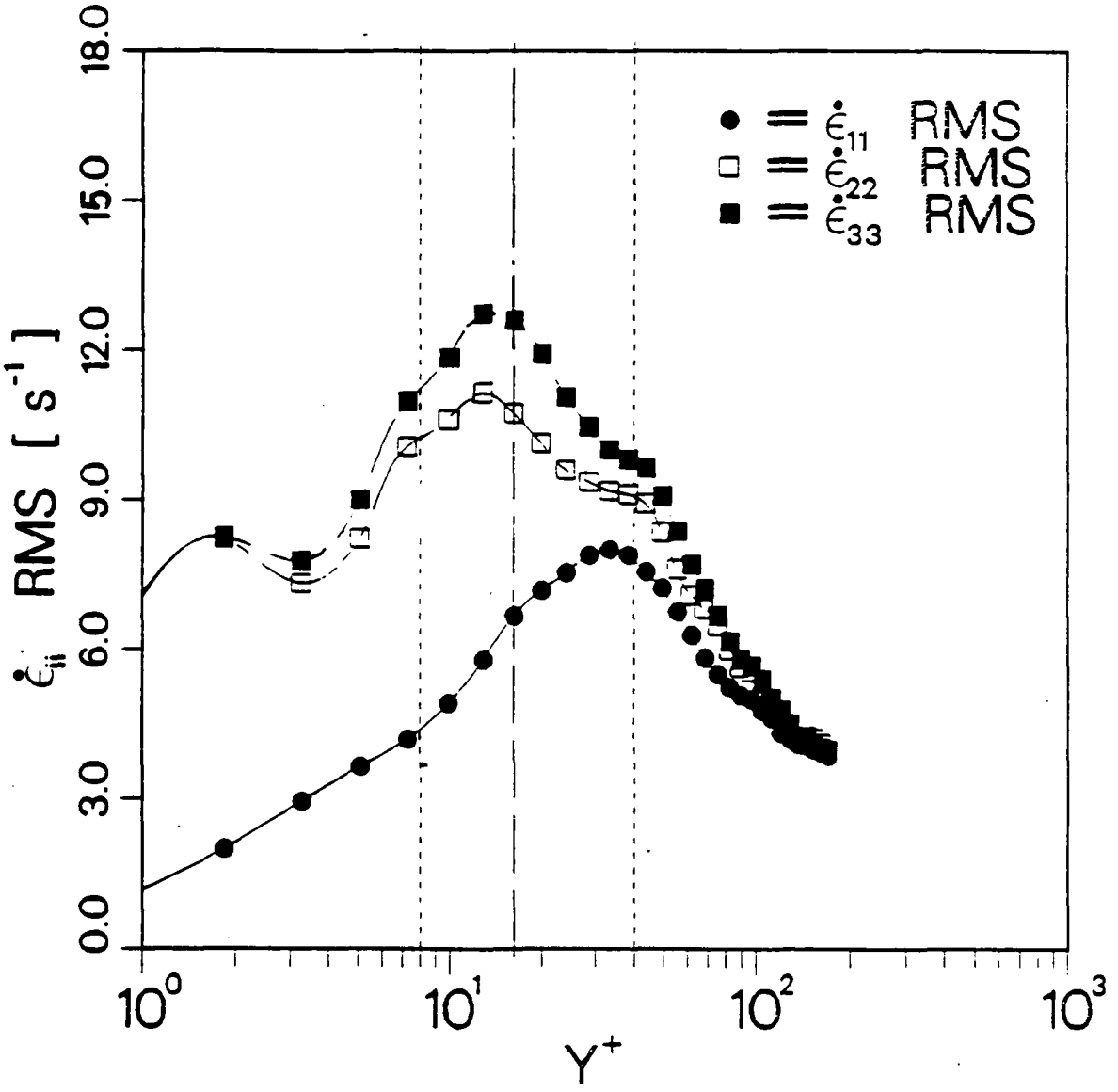

Figure 14. Elongation Rates Across a Turbulent Channel.

Root-mean-square elongation rates across a channel of infinite planar extent. Results are from a direct numerical simulation of Newtonian flow at Re = 3900. Data is scaled to channel width of 2.54 cm. The buffer region is between the short-dashed lines. The different components correspond to: 11 - streamwise, 22 - wall-normal, and 33 - spanwise.

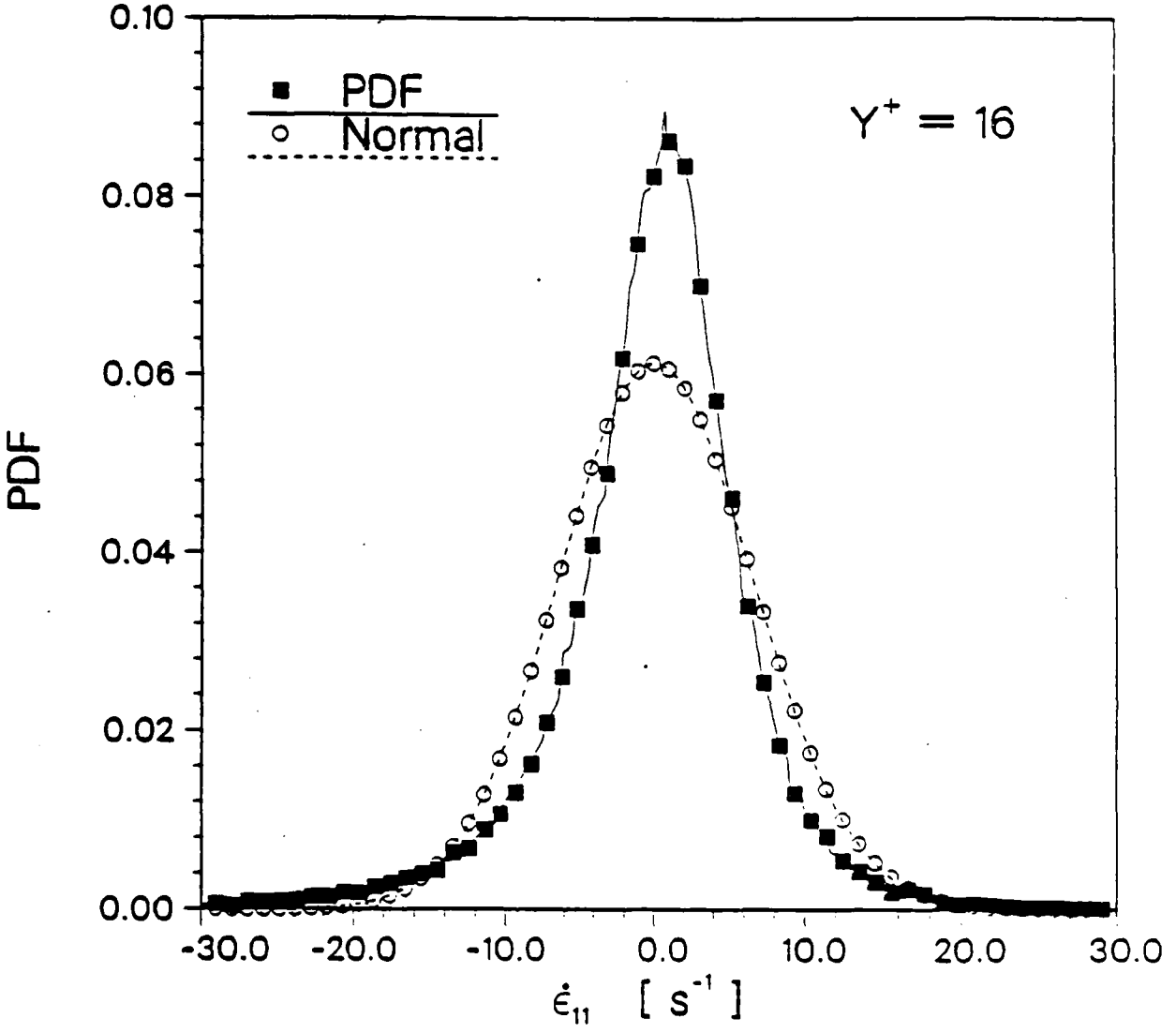

Figure 15. Probability Density Function of the Streamwise Elongation Rate.

Results are from a direct numerical simulation of Newtonian flow at Re = 3900. Data is scaled to channel width of 2.54 cm and represents values at a distance from the wall of 16 viscous units. The PDF is shown as the solid squares. A normal distribution with the same mean and standard deviation is shown as the hollow circles.

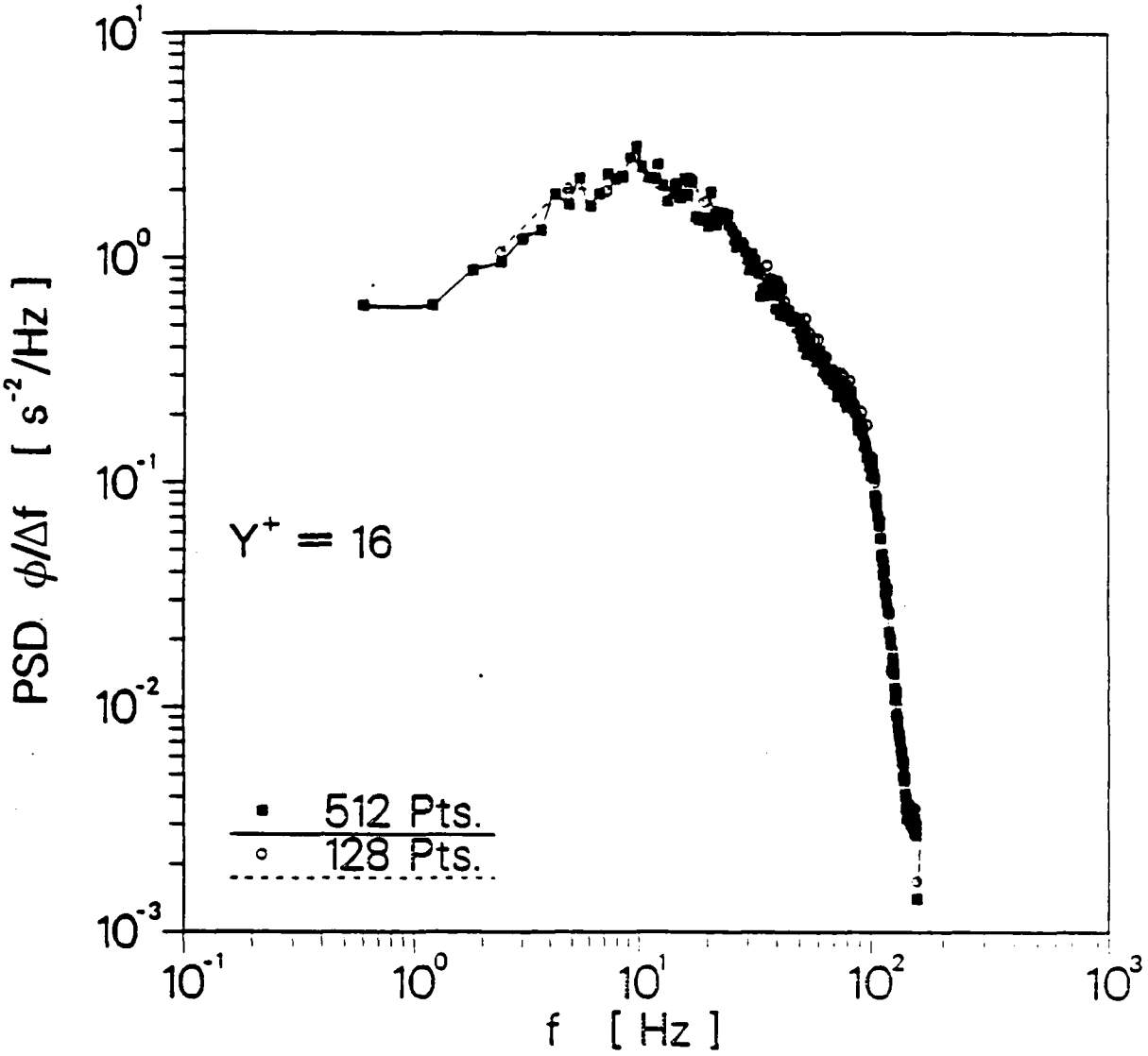

Figure 16. Power Spectral Density of the Streamwise Elongation Rate.

Results are from a direct numerical simulation of Newtonian flow at Re = 3900. Data is scaled to channel width of 2.54 cm and represents values at a distance from the wall of 16 viscous units. The PSD is shown as the solid squares.

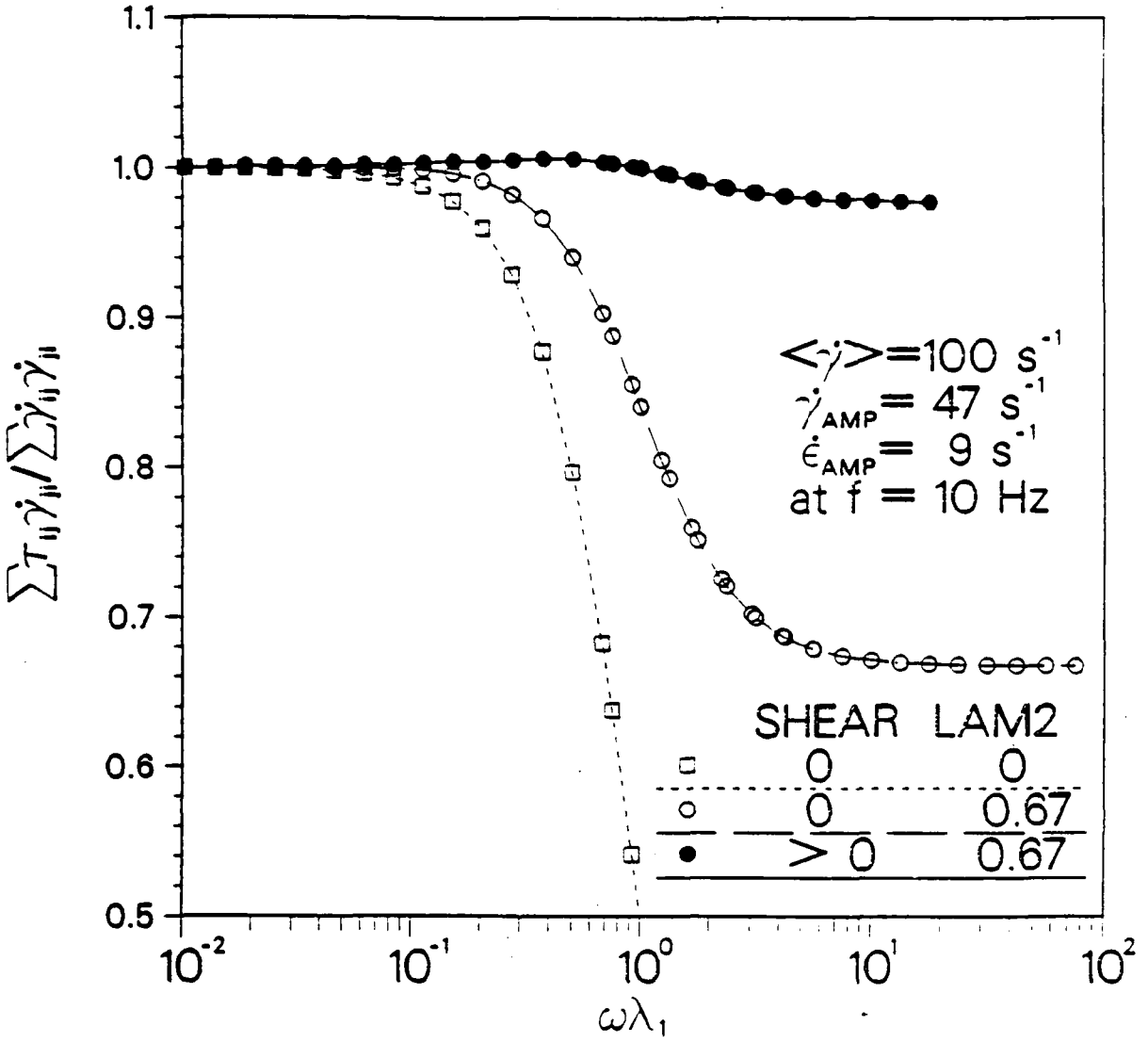

Figure 17. Ratio of Energy Dissipation of Oldroyd-B Model to Newtonian Fluid.

Flow field is a fluctuating, homogeneous flow. The energy dissipation is plotted as a function of frequency times relaxation time. The magnitudes of the mean shear rate, oscillating shear rate, and oscillating elongation rate scale with the product of the relaxation time and the frequency of both oscillations. The mean shear is 100 1/s, oscillating shear is 47 1/s, and the oscillating elongation is 9 1/s at a frequency of 10 Hz. The dissipation with a mean shear and a retardation time of 2/3 is shown by the solid circles, dissipation with zero mean shear and a retardation time of 2/3 is shown by the hollow circles, and dissipation with zero mean shear and zero retardation time is shown by the hollow squares.

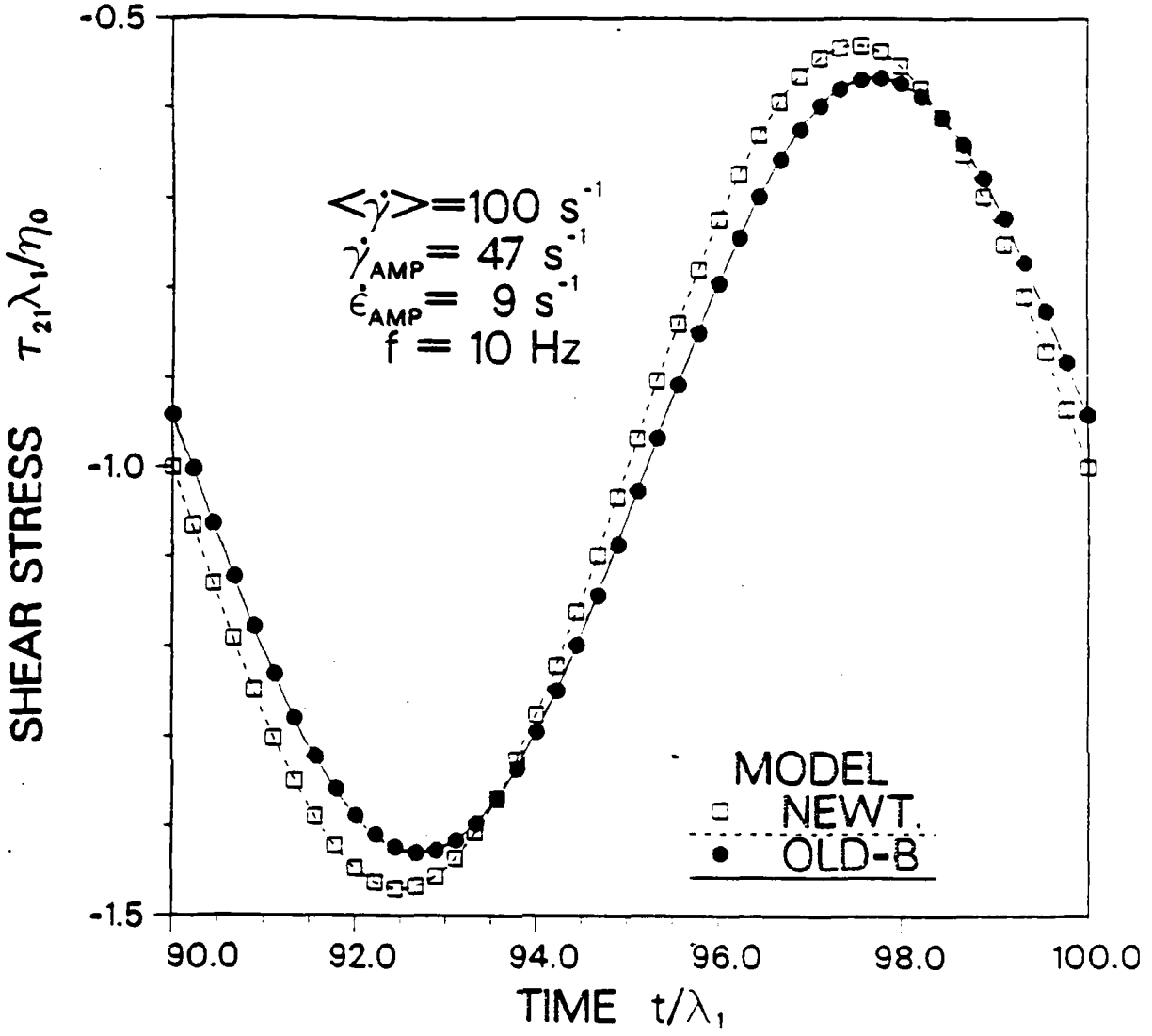

Figure 18. Shear Stress As a Function of Time.

Flow field is a fluctuating, homogeneous flow. The amplitudes of the mean shear rate, oscillating shear rate, oscillating elongation rate are 100, 47, and 9 1/s, respectively. The frequency of both oscillations is 10 Hz. The relaxation time of the Oldroyd-B model is 10 ms, and the ratio of the retardation to relaxation times is 2/3. The shear stress of the Oldroyd-B is shown by the soid circles, and the same stress of the Newtonian fluid is shown by the hollow squares.

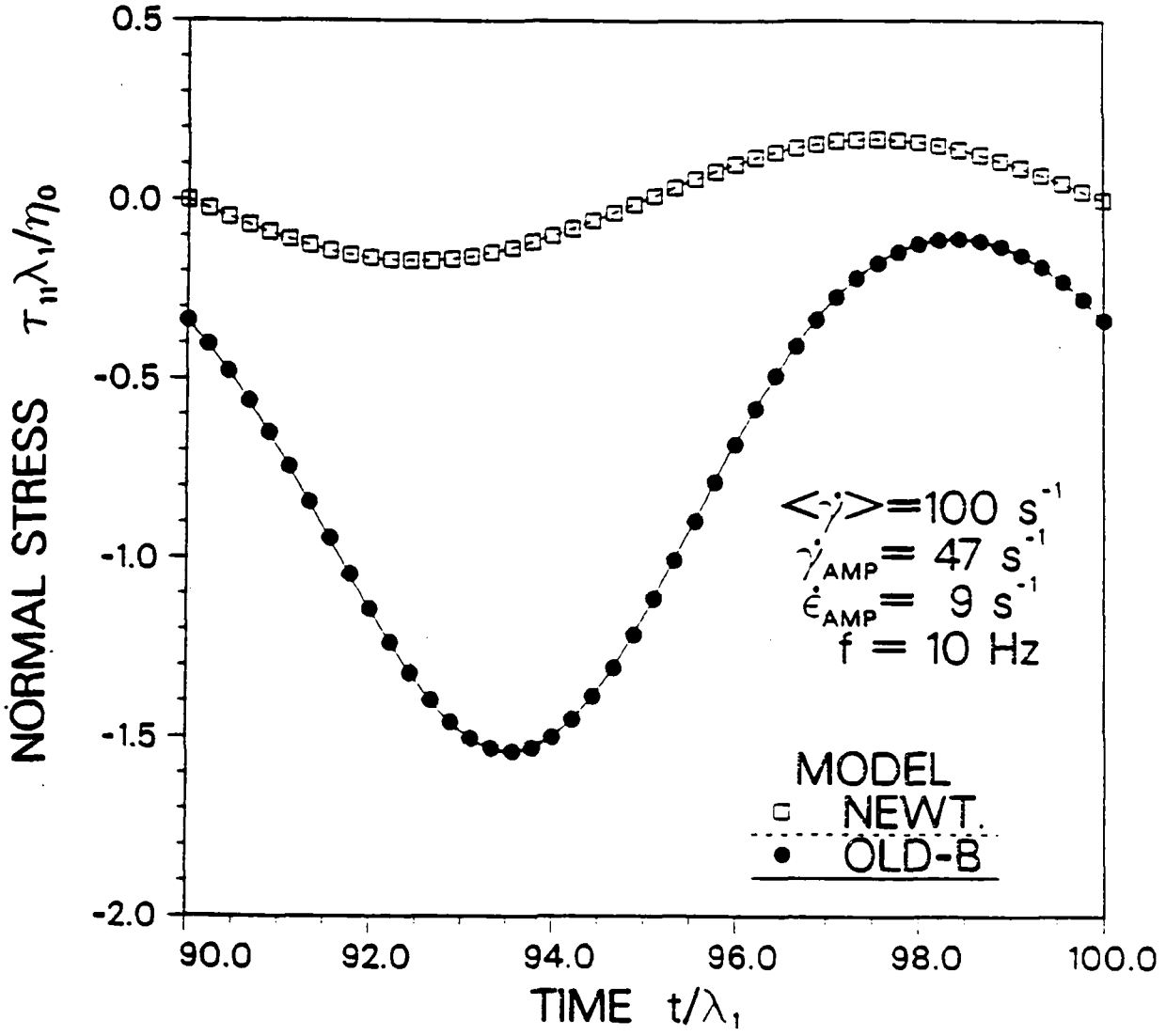

Figure 19. Normal Stresses As a Function of Time.

Flow field is a fluctuating, homogeneous flow. The amplitudes of the mean shear rate, oscillating shear rate, oscillating elongation rate are 100. 47. and 9 1/s. respectively. The frequency of both oscillations is 10 Hz. The relaxation time of the Oldroyd-B model is 10 ms, and the ratio of the retardation to relaxation times is 2/3. The streamwise normal stress of the Oldroyd-B is shown by the soid circles. and the same stress of the Newtonian fluid is shown by the hollow squares.

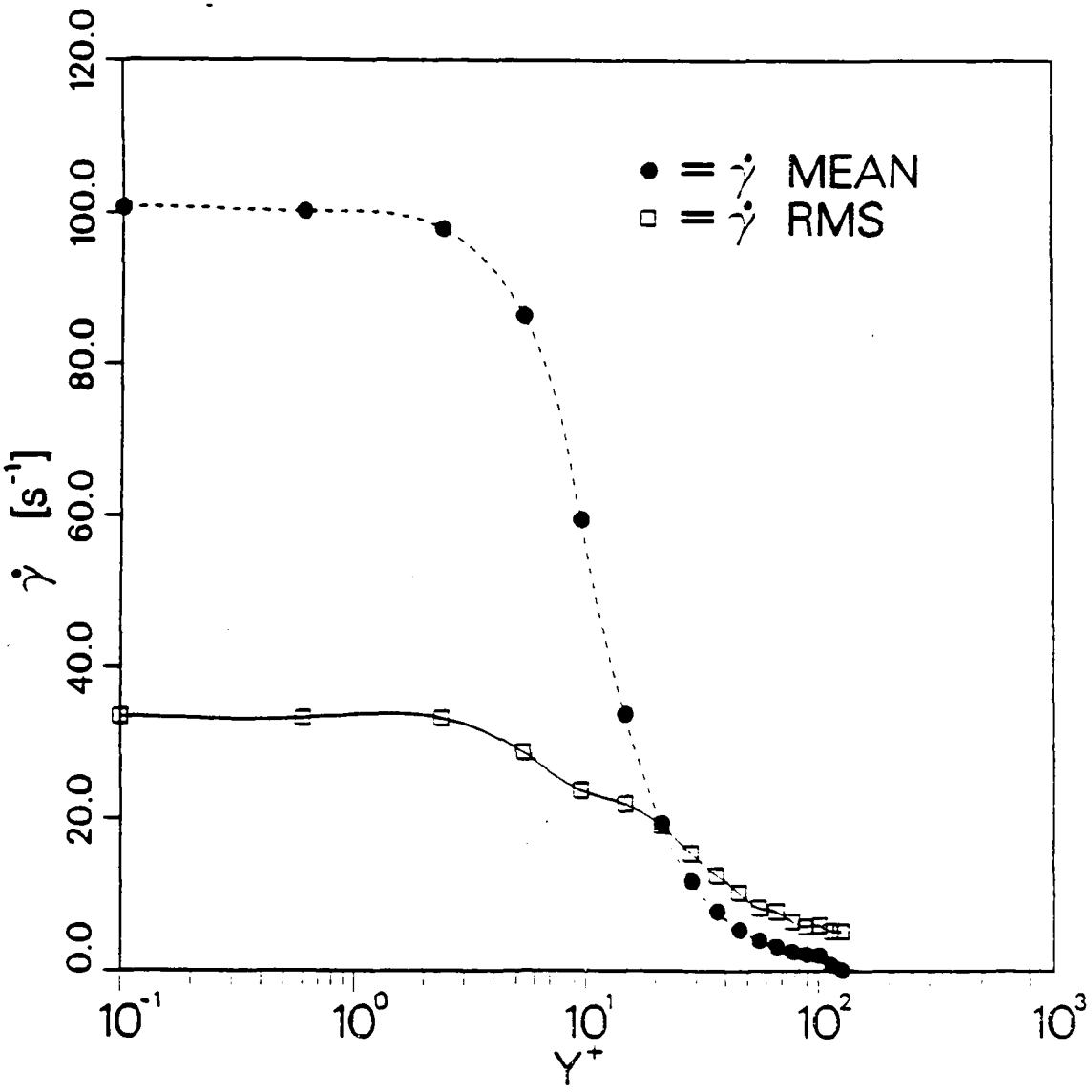

Figure 20. Shear Rate Across a Turbulent Channel.

Mean and root-mean-square shear rate across a channel of infinite planar extent. Results are from a direct numerical simulation of Newtonian flow at Re = 2130. Data is scaled to channel width of 2.54 cm.

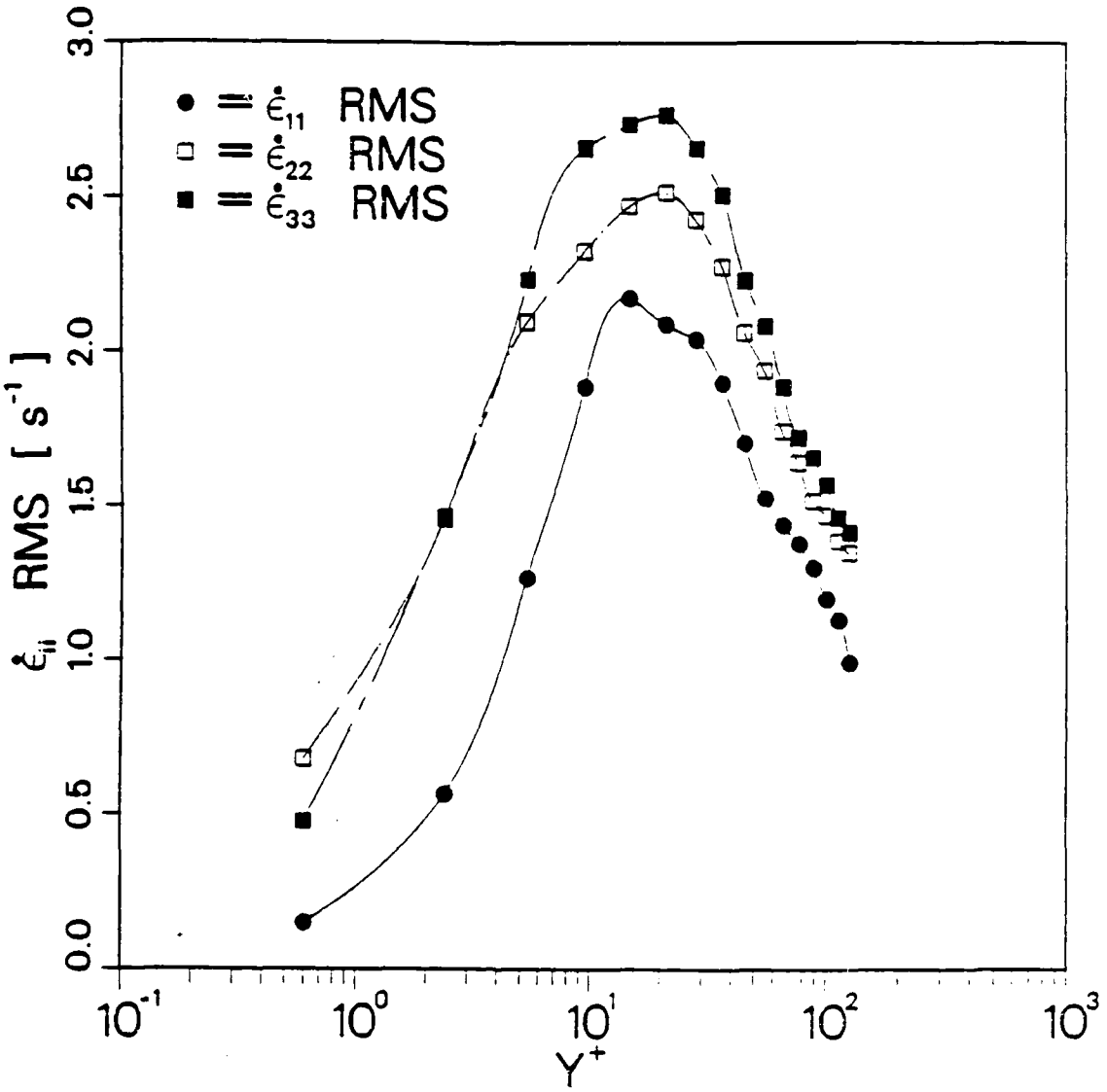

Figure 21. Elongation Rates Across a Turbulent Channel.

Root-mean-square elongation rates across a channel of infinite planar extent. Results are from a direct numerical simulation of Newtonian flow at Re = 2130. Data is scaled to channel width of 2.54 cm. The different components correspond to: 11 – streamwise, 22 – wall-normal, and 33 – spanwise.

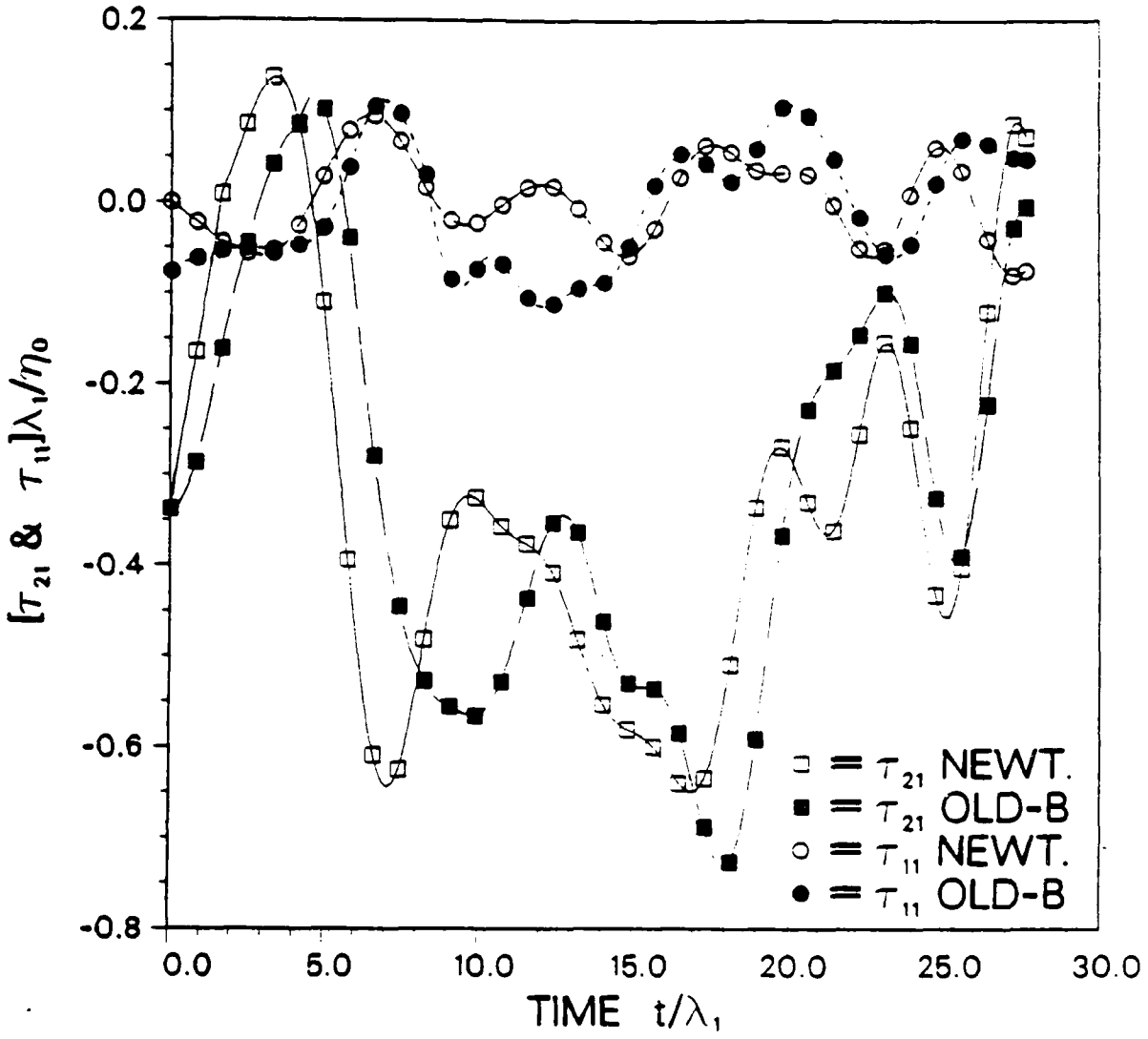

Figure 22. Turbulent Stresses As a Function of Time.

The shear and streamwise component of the normal stress of an Oldroyd-B model and a Newtonian fluid are estimated as a function of time. The stresses are obtained by integrating the constitutive equation at one point from deformations of a Newtonian turbulence direct simulation at Re = 2130. The point chosen is 15 viscous units away from the wall. The curves for the shear stress are: Oldroyd-B (solid squares) and Newtonian (hollow squares). The curves for the normal stress are: Oldroyd-B (solid circles) and Newtonian (hollow circles). The assumed parameters for the Oldroyd-B model are a relaxation time of 10 ms and a ratio of retardation time to relaxation time of 2/3.

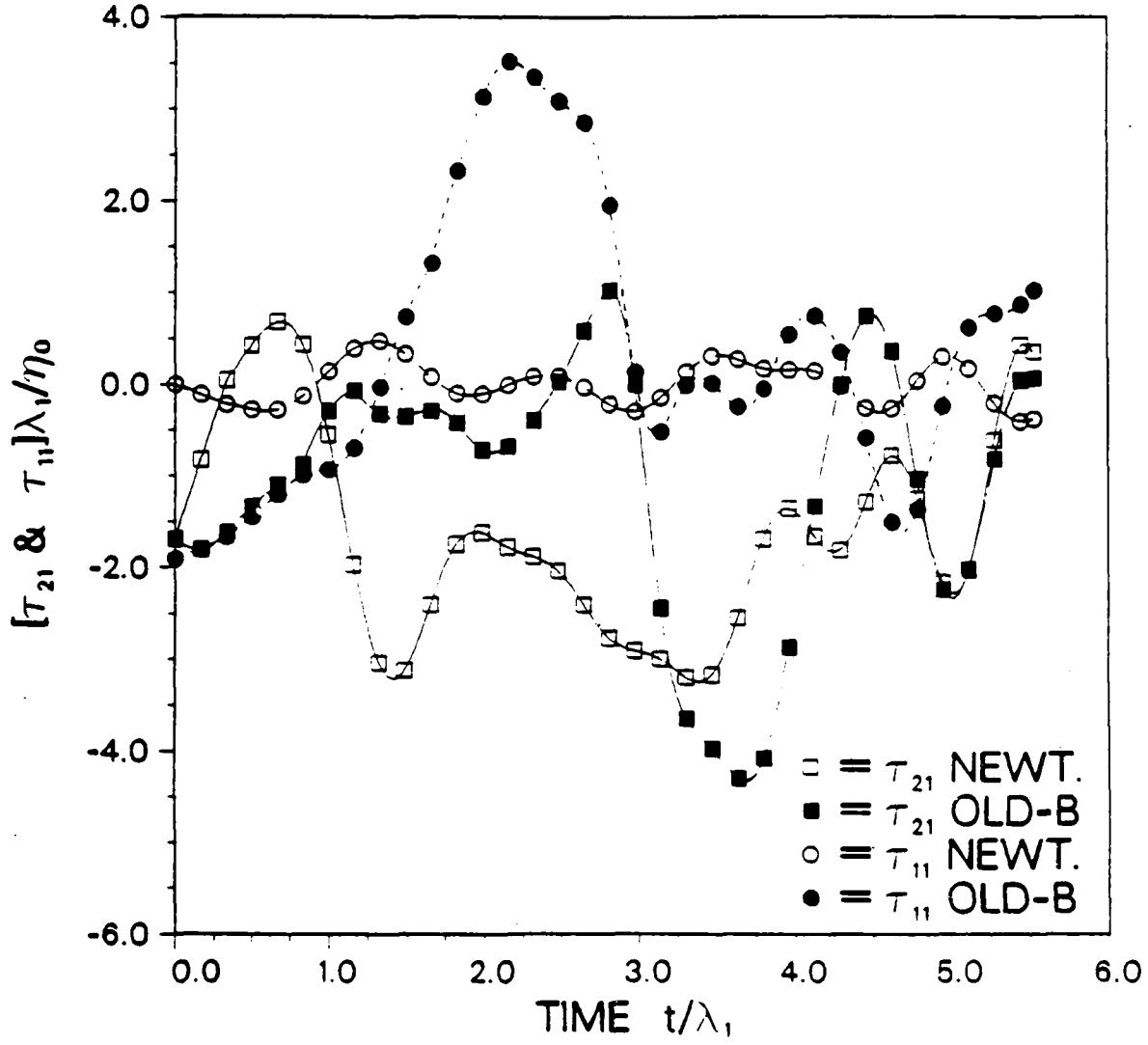

Figure 23. Turbulent Stresses As a Function of Time.

The shear and streamwise component of the normal stress of an Oldroyd-B model and a Newtonian fluid are estimated as a function of time. The stresses are obtained by integrating the constitutive equation at one point from deformations of a Newtonian turbulence direct simulation at Re = 2130. The point chosen is 15 viscous units away from the wall. The curves for the shear stress are: Oldroyd-B (solid squares) and Newtonian (hollow squares). The curves for the normal stress are: Oldroyd-B (solid circles) and Newtonian (hollow circles). The assumed parameters for the Oldroyd-B model are a relaxation time of 50 ms and a ratio of retardation time to relaxation time of 2/3.